Journal of Medicinal Chemistry

Article

Discovery of a Potent, Selective T-type Calcium Channel Blocker as a Drug Candidate for the Treatment of Generalized Epilepsies

Olivier Bezençon, Bibia Heidmann, Romain Siegrist, Simon Stamm, Sylvia Richard, Davide Pozzi, Olivier Corminboeuf, Catherine Roch, Melanie Kessler, Eric A. Ertel, Isabelle Reymond, Thomas Pfeifer, Ruben de Kanter, Michael Toeroek-Schafroth, Luca G. Moccia, Jacques Mawet, Richard Moon, Markus Rey, Bruno Capeleto, and Elvire Fournier

Just Accepted

ACS Publications

1
2
3
4
5
6
7
8
9
10
11
12
13
14
15
16
17
18
19
20
21
22
23
24
25
26
27
28
29
30
31
32
33
34
35
36
37
38
39
40
41
42
43
44
45
46
47
48
49
50
51
52
53
54
55
56
57
58
59
60

Discovery of a Potent, Selective T-type Calcium Channel Blocker as a Drug Candidate for the Treatment of Generalized Epilepsies

Olivier Bezençon*, Bibia Heidmann, Romain Siegrist, Simon Stamm, Sylvia Richard, Davide Pozzi, Olivier Corminboeuf, Catherine Roch, Melanie Kessler, Eric A. Ertel, Isabelle Reymond, Thomas Pfeifer[†], Ruben de Kanter, Michael Toeroek-Schafroth, Luca G. Moccia, Jacques Mawet, Richard Moon, Markus Rey, Bruno Capeleto, and Elvire Fournier

Chemistry, Biology and Pharmacology & Pre-clinical development, Drug Discovery, Idorsia Pharmaceuticals Ltd, Hegenheimermattweg 91, CH – 4123 Allschwil

KEYWORDS: T-type calcium channels; epilepsy; Ames test; clinical candidate.

ABSTRACT: We report here the discovery and pharmacological characterization of *N*-(1-benzyl-*1H*-pyrazol-3-yl)-2-phenylacetamide derivatives as potent, selective, brain-penetrating T-type calcium channel blockers. Optimization focused mainly on solubility, brain penetration, and search for an aminopyrazole metabolite that would be negative in an *Ames* test. This resulted in the preparation and complete characterization of compound **66b** (ACT-709478), which has been selected as clinical candidate.

1
2
3
4
5
6
7
8
9
10
11
12
13
14
15
16
17
18
19
20
21
22
23
24
25
26
27
28
29
30
31
32
33
34
35
36
37
38
39
40
41
42
43
44
45
46
47
48
49
50
51
52
53
54
55
56
57
58
59
60

INTRODUCTION

T-type calcium channels (TTCCs) belong to the family of the low-voltage-activated calcium channels. These channels are the products of three genes, CACNA1G, CACNA1H, and CACNA1I , yielding the $Ca_v3.1$, $Ca_v3.2$, and $Ca_v3.3$ channels, respectively. While the $Ca_v3.1$- and $Ca_v3.2$-channels are expressed in several organs, in particular the heart and the brain[1], the $Ca_v3.3$ channel seems to be exclusively expressed in the brain. The therapeutic potential of a TTCC blocker for cardiovascular diseases led to the development of weak, non-selective compounds, whose physicochemical properties resulted in a poor brain penetration[2]. On the other hand, the discovery and development of potent, selective, brain penetrant TTCC blockers has been the result of more recent research. It should be noted that throughout the manuscript, the term *selective blockers* is used for compounds that block the three TTCCs, $Ca_v3.1$, $Ca_v3.2$, and $Ca_v3.3$ with similar potencies, while being much less potent toward any other target, in particular $Ca_v1.2$.

The belated discovery of potent, selective TTCC blockers might be linked to difficulties in cloning these channels, and to the absence of high throughput screening techniques for these targets until recently. Indeed, while high throughput screening assays, like FLIPR assays, have been known for many years in the field of G-protein-coupled receptors (GPCRs) for instance, the search for voltage gated channel blockers relied for years solely on the low throughput patch-clamp technique. With the development of automated patch-clamp techniques in the early 2000s, the throughput increased slightly but it has been only recently that high-throughput colorimetric assays were developed to measure the activity of voltage-gated calcium channels.[3]
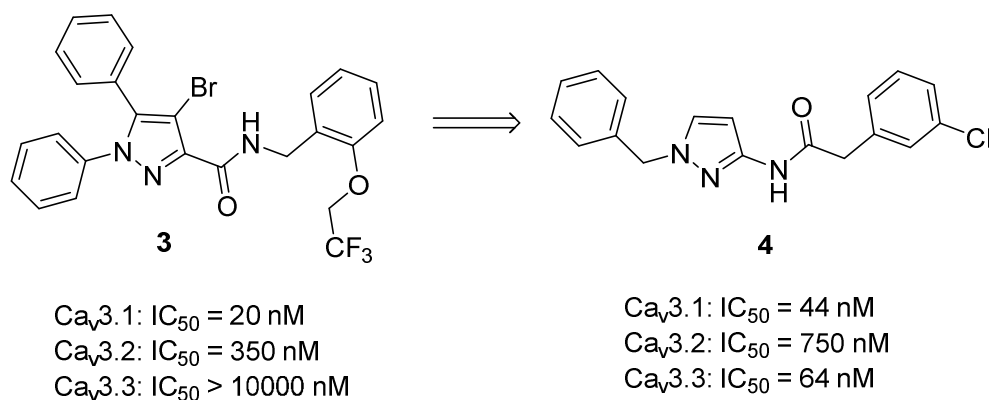
The discovery of TTCC blockers followed this evolution. Mibefradil (**1**, Fig. 1), discovered in the early 1990s in a phenotypic manner, was considered for many years as the prototypic TTCC blocker. On the other hand, this compound is not brain-penetrant, and blocks multiple channels. In our hands, compound **1** blocked $Ca_v3.1$, $Ca_v3.2$, $Ca_v3.3$, $Ca_v1.2$, and hERG with IC_{50}-values of 64 nM, 130 nM, 130 nM, 250 nM, and 580 nM, respectively. Literature data shows that this compound also blocks $Ca_v2.2$ (IC_{50}-values between 1000 and 3000 nM)[4], as well as $Na_v1.5$, $Na_v1.4$, $Na_v1.2$, and $Na_v1.7$[5] (IC_{50}-values between 500 and 2000 nM). Many years later, two selective, brain-penetrant TTCC blockers, MK-8998 (**2a**) and Z-944 (**2b**), entered clinical trials.[6] More recently, CX-8998 and CX-5395 (structures unknown) were claimed to be new TTCC blockers in clinical trials[7]. A few model compounds were shown to be efficacious in animal models for generalized epilepsy[8], insomnia[9], schizophrenia[6a, 10], Parkinson[11], essential tremor[8f, 12], and obesity[13]. Compound **2b** shows efficacy in preclinical pain models[14]. The potential therapeutic benefit of a TTCC blocker in absence epilepsies is supported by genetic, functional or pharmacological evidence. All TTCCs are expressed in the neuronal network involved in the generation of the spike-and-wave discharges, which is the hallmark of absence seizures[15]. Mutations in the genes expressing $Ca_v3.1$ or $Ca_v3.2$ have been described both in human and animal models of absence epilepsy or other forms of idiopathic generalized epilepsies[16]. Most mutations in $Ca_v3.2$ were described as gain-of-function mutations due to an increase of intrinsic activity of the channels or to an increase of trafficking of the channels to the plasma membrane. $Ca_v3.1$ overexpression or, in contrast, knockout, was shown to modulate the generation of spike-and-wave discharges in mice[17]. Less is know regarding the role of $Ca_v3.3$.
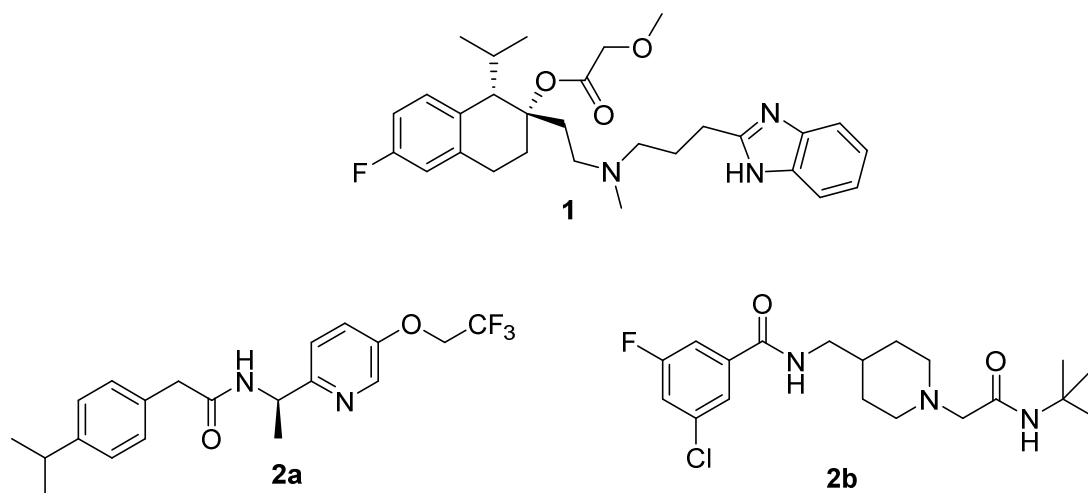
Figure 1. Structures of **1**, **2a** , and **2b**

Different classes of TTCC blockers that were studied in our laboratories were presented elsewhere[8a, 8b]. In particular, we found that pyrazole 3-carboxamides are subtype-selective $Ca_v3.1$ blockers, as exemplified by the derivative **3**[18] (Fig. 2). Along structure activity relationship (SAR) studies, we prepared the corresponding inverse amides, starting with a focused library of amide couplings based on commercially available 3-aminopyrazoles, and we identified compound **4** as a moderately potent TTCC blocker ($IC_{50} \sim$ 40-800 nM) with some selectivity versus $Ca_v1.2$ channels (IC_{50} = 2800 nM). Compound **4**, with a molecular weight of 326 g/mol, a clogP of 3.2, a polar surface area of 47 $Å^2$, and a ligand efficiency of 0.44 on $Ca_v3.1$, represented an acceptable starting point in the search for TTCC blockers. Starting from this compound, we aimed at identifying a compound that could be selected as a preclinical candidate for later treatment of generalized epilepsies in human. In a particular, beside a standard safety profile, we wanted to develop a compound blocking all three TTCCs with similar potencies, with an excellent efficacy in animal models at low dose, and suitable for a once a day dosing in human. In this article, we describe our efforts in optimizing this series of aminopyrazole amides,

eventually leading to the identification of the clinical candidate **66b** (*N*-(1-((5-cyanopyridin-2-yl)methyl)-1*H*-pyrazol-3-yl)-2-(4-(1-(trifluoromethyl)cyclopropyl)phenyl)acetamide, ACT-709478). On our way to this optimized compound, we had to adjust polarity to maintain solubility without promoting active transport. Furthermore, we had to go through an extensive optimization of the aminopyrazole in order to identify an *Ames* negative aromatic amine that was formed after hydrolysis of the amide bond in plasma.


3

Ca$_v$3.1: IC$_{50}$ = 20 nM
Ca$_v$3.2: IC$_{50}$ = 350 nM
Ca$_v$3.3: IC$_{50}$ > 10000 nM

4

Ca$_v$3.1: IC$_{50}$ = 44 nM
Ca$_v$3.2: IC$_{50}$ = 750 nM
Ca$_v$3.3: IC$_{50}$ = 64 nM

Figure 2. A first identified aminopyrazole derivative

RESULTS AND DISCUSSION

Initial SAR studies. From compound **4**, we started investigating the SAR at the phenylacetic acid moiety. Compounds **5a** – **5l** (Table 1) were prepared by amide coupling between a phenylacetic derivative, and an aminopyrazole, prepared from nitropyrazole in two steps (see supporting information). Derivative **5a**, bearing a non-substituted phenyl group, was less potent than compound **4**, whereas a position screen with a methyl group led to an excellent gain in potency at the *para*-position (compound **5b**). Substituting the *meta*-position (compound **5c**) was of secondary importance, and substituting the *ortho*-position (compound **5d**) had a minor influence only. The nature of the *para*-substituent did not seem to play a crucial role (compounds

5f to **5k**), although an electrodonating methoxy substituent led to some loss in potency (compound **5e** vs. **5b**). The longer electrodonating ethoxy- and trifluoromethoxy groups led to the compounds **5f** and **5g**, equipotent to compound **5b**. An electrowithdrawing chlorine atom (compound **5h**) was tolerated as well. Incorporation of an isopropyl- or a dimethylamino group in the *para*-position (compounds **5i** and **5j**) led to potent blockers. Also, the moderate potency of compound **5e** was greatly improved by introducing additionally a *meta*-methyl substituent (compound **5k**). Finally, a benzoic acid substituent as replacement for the phenylacetic acid moiety led to completely inactive compound **5l**.

**Table 1.** Potency of aminopyrazoles on TTCCs

5a - 5k   5l
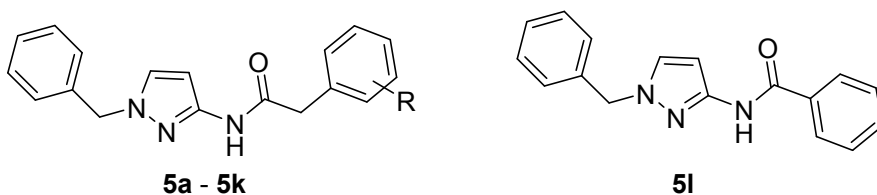
Compound	R	$Ca_v3.1$ IC_{50} in nM^a	$Ca_v3.2$ IC_{50} in nM^a	$Ca_v3.3$ IC_{50} in nM^a
5a	H-	*1140*	*>10000*	*390*
5b	*p*-Me-	35	210 (52-1100)	18 (9.0-34)
5c	*m*-Me-	54	1040 (260-5800)	67 (26-200)
5d	*o*-Me-	490	3400	120
5e	*p*-MeO-	170	610	32
5f	*p*-EtO-	35	210	25
5g	*p*-CF$_3$O-	13 (4.0-61)	155 (88-310)	15 (9.0-28)
5h	*p*-Cl-	41	280	24
5i	*p*-^{i}Pr-	5.1 (3.7-7.7)	23 (10-91)	7.6 (3.5-26)

5j	*p*-Me₂N-	14 (13-17)	38 (37-68)	2.9 (2.8-37)
5k	*p*-MeO-*m*-Me-	11 (5.0-24)	57 (14-300)	6.5
5l	-	*>10000*	*>10000*	*>10000*

^{a}IC$_{50}$ values based on single measurements are indicated in italics, other IC$_{50}$ values are the geometric mean of at least two measurements. Where sufficient data were available for calculation 95% confidence intervals are indicated in parenthesis. Data were obtained with a Fluorescence Imaging Plate Reader (FLIPR$^®$) assay, see supporting information for details.

We then turned our attention to the *N*-benzyl substituent attached to the pyrazole ring (Table 2). A position screen with a methyl group demonstrated that the *ortho*-position should not be substituted (compound **6a** vs. **5j**), while substitution was tolerated at the *meta*-position (compound **6b**) and beneficial at the *para*-position (compound **6c**). Focusing on the *para*-position, we found that electrowithdrawing substituents (compounds **6d**, **6e**, **6g**) as well as electrodonating groups (compounds **6f**, **6h**, **6i**) were tolerated. Especially, very potent compounds were obtained with a halogen at this position. Combining substituents at the *para*- and *meta*-positions led to very potent derivatives like the compounds **6j**, **6k**, and **6l**. In contrast, *para*-substitution with hydrogen bond donors or acceptors (compounds **6m** and **6n**) was not tolerated. Also, as for the other end of the molecule, replacement of the benzyl by a phenyl was detrimental to the potency (compound **6o**).

Table 2. Potency of aminopyrazoles on TTCCs

6a - **6n**   **6o**
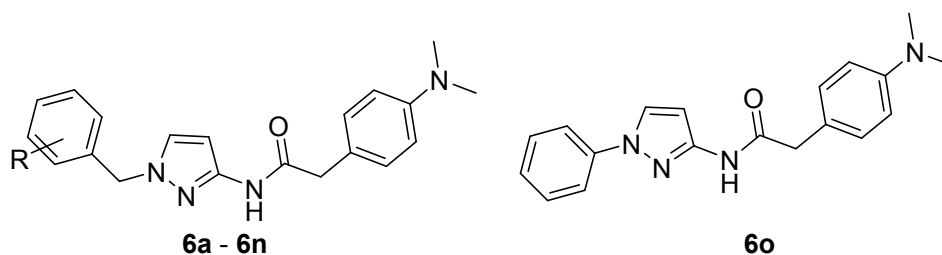
Compound	R	$Ca_v3.1$ IC_{50} in nM^a	$Ca_v3.2$ IC_{50} in nM^a	$Ca_v3.3$ IC_{50} in nM^a
6a	*o*-Me-	250 (150-420)	190 (21-3400)	40 (19-88)
6b	*m*-Me-	8.1 (4.1-16)	36 (6.0-340)	2.8 (1.1-7.2)
6c	*p*-Me-	7.0 (4.5-11)	10 (3.2-40)	1.8 (1.8-3.2)
6d	*p*-Cl-	1.1 (0.5-2.2)	4.1 (0.3-93)	1.1 (0.3-4.8)
6e	*p*-F-	4.2 (2.0-10)	12 (3.3-93)	2.0 (0.8-6.8)
6f	*p*-MeO-	23 (14-41)	47 (10-570)	3.4 (2.7-4.2)
6g	*p*-CN-	11 (5.4-32)	20 (11-44)	3.5 (2.0-6.8)
6h	*p*-F_2HCO-	6.8 (2.5-21)	10 (7.2-15)	1.6 (1.2-2.1)
6i	*p*-F_3CO-	2.2 (1.7-2.8)	5.1 (1.6-18)	1.0 (0.8-1.2)
6j	3,4-diF-	1.5 (1.0-2.5)	3.4 (2.3-4.0)	0.89 (0.7-1.3)
6k	3,5-diF-4-MeO-	3.2 (1.7-6.3)	7.8 (0.3-690)	0.92 (0.4-2.7)
6l	*m*-F-*p*-CN-	3.1 (1.5-7.8)	14 (8.1-27)	1.8 (1.3-2.7)
6m	*p*-CH_3CONH-	*>10000*	*>10000*	*3300*
6n	*p*-(2-oxopyrrolidin-1-yl)	*5700*	*>10000*	*520*
6o	-	*1400*	*6300*	*2300*

^{a}IC_{50} values based on single measurements are indicated in italics, other IC_{50} values are the geometric mean of at least three measurements, 95% confidence intervals are indicated in parenthesis. Data were obtained with a Fluorescence Imaging Plate Reader (FLIPR$^®$) assay, see supporting information for detail.

Characterization of a first model compound. At this stage, we selected compound **6j** for further characterization. Compound **6j** appeared to be selective for TTCCs, being a weak blocker of $Ca_v1.2$-channels (IC_{50} = 7100 nM), and of sodium and potassium channels in rat cortical

neurons (< 15% and <25% block at 10 μM, respectively). Aqueous solubility was low (3 mg/L at pH 7), whereas solubility in fasted, respectively fed state simulated intestinal fluid (FaSSIF, resp. FeSSIF) remained acceptable (9 and 31 mg/L, resp.), a common characteristic for this series of compounds. Other ADME parameters were promising, especially with an intrinsic clearance of 41 μL/min/mg protein in human microsomes and 360 μL/min/mg protein in rat microsomes. In this regard, the presence of a *para* substituent at the phenylacetyl moiety did not only increase potency, it also dramatically stabilized compounds against oxidative metabolism in rat liver microsomes. Finally, compound **6j** was well permeable in vitro without being a Pgp substrate (in MDR1-MDCK cells $P_{appA \rightarrow B} = 62 \cdot 10^{-6}$ cm/s; ratio B→A/A→B = 0.9). We then administered this compound or matching vehicle in a cross-over design by oral gavage at the beginning of the night active period to Wistar Albino Glaxo Rats of Rijswijk (WAG/Rij rats), a model of generalized non-convulsive absence like epilepsy[19]. These rats had been previously implanted with telemetry transmitters allowing continuous recording of the spontaneous seizures by electroencephalogram (EEG) in freely moving undisturbed animals. Over the following 12-h period, 10 mg/kg of **6j** completely suppressed seizures ($p < 0.001$, paired t-test) (Fig. 3a). Brain concentrations of **6j** were measured in normal Wistar rats 1 h after the same dose: total and free concentrations were 1703 ± 415 nM, and 22 ± 5 nM, respectively ($f_{u,brain} = 0.013$). At that time point, free brain concentrations were 6-fold to 25-fold above the IC_{50}-values measured on the TTCCs, suggesting that the channels are well inhibited during a significant fraction of the 12-h EEG recording.
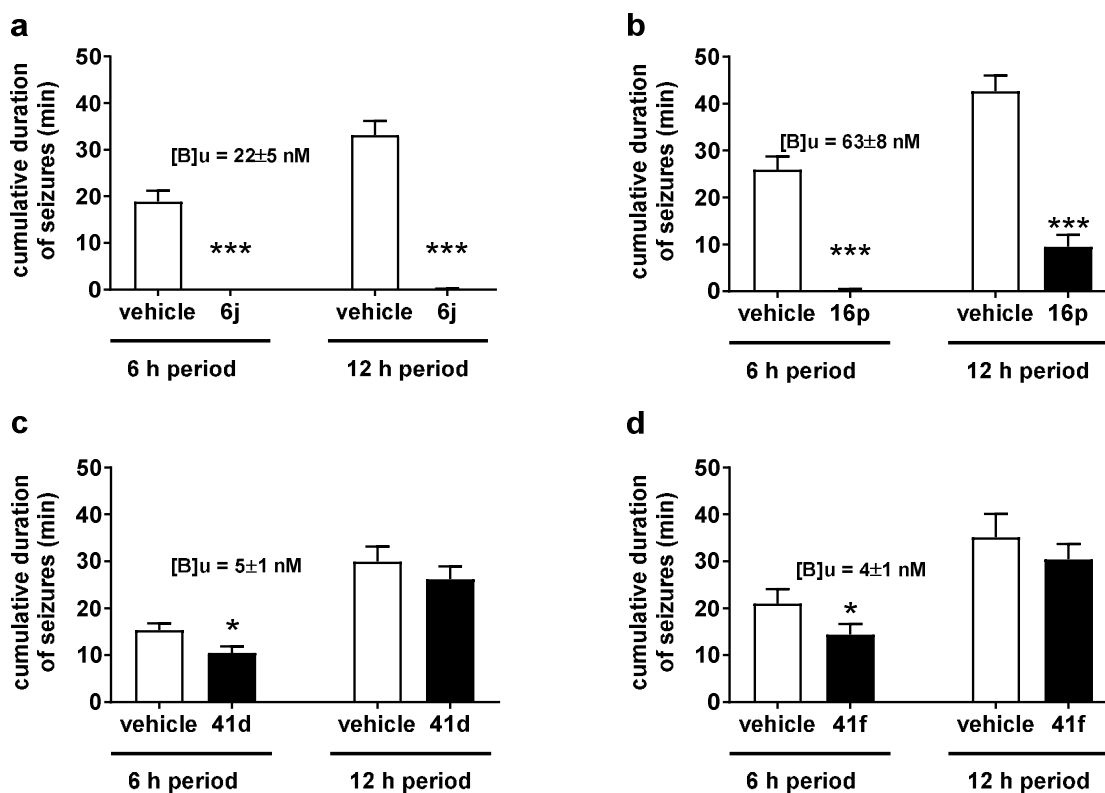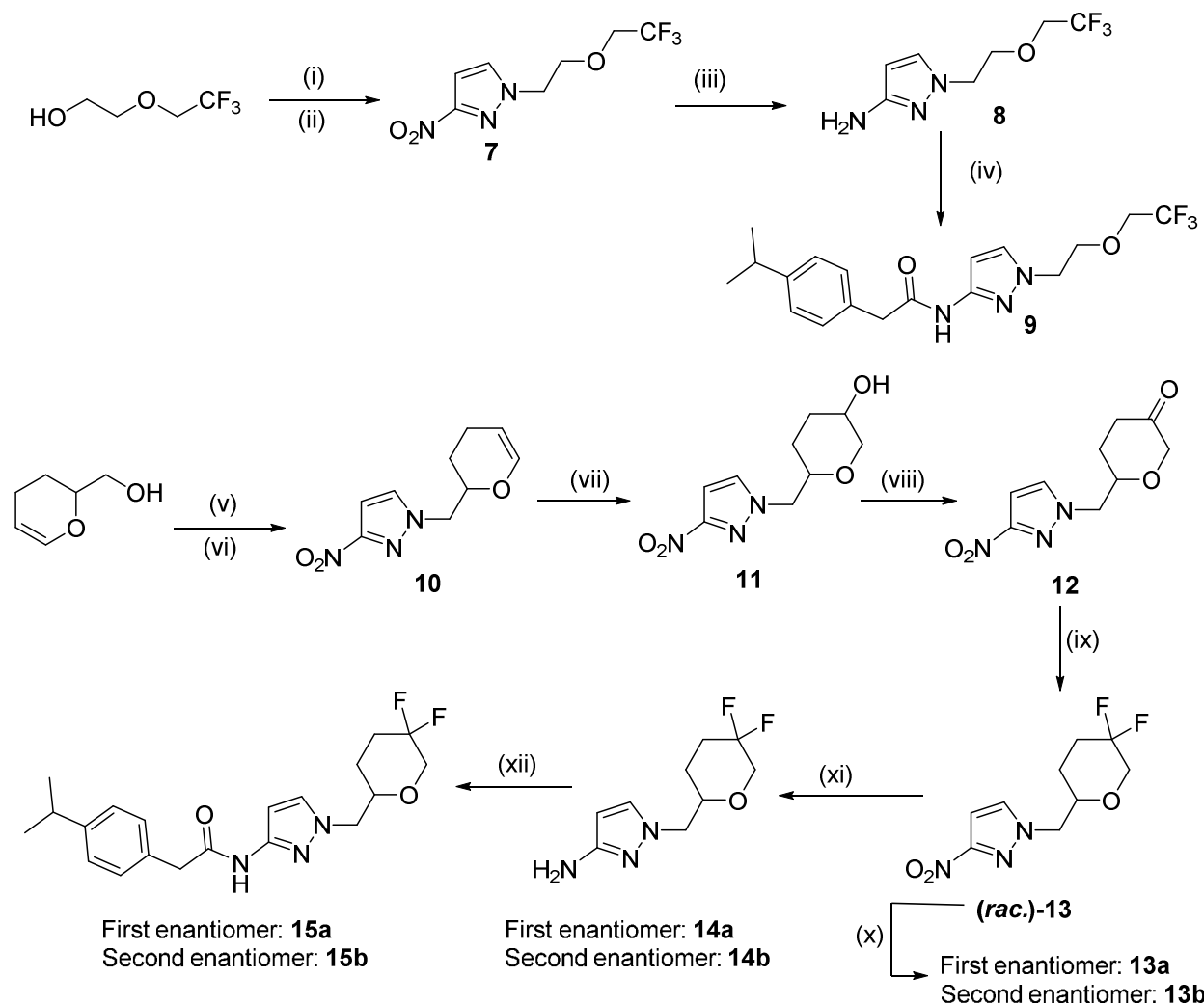
Figure 3. Impact of compounds **6j** (a), **16p** (b), **41d** (c) or **41f** (d) at 10 mg/kg *po* on the cumulative duration of absence seizures in male WAG/Rij rats over the first 6 h or the first 12 h night periods following administration. Data are expressed as mean ± SEM (n = 6 to 8 per group); *, $p < 0.05$; ***, $p < 0.001$ compared to vehicle (10% PEG400 + 90 % MC 0.5%) treated rats (paired t-test); [B]u = free brain concentration 1 h post administration in normal Wistar rats (mean ± SD, n = 3). Baseline values (in min) for (a) 6 h period, **6j**, 20 ± 1 vs. veh., 19 ± 1; 12 h period, **6j**, 37 ± 2 vs. veh., 35 ± 2; (b) 6 h period, **16p**, 29 ± 2 vs. veh., 27 ± 8; 12 h period, **16p**, 46 ± 2 vs. veh., 43 ± 6; (c) 6 h period, **41d**, 17 ± 1 vs. veh., 19 ± 2; 12 h period, **41d**, 32 ± 3 vs. veh., 34 ± 3; (d) 6 h period, **41f**, 20 ± 2 vs. veh., 21 ± 1; 12 h period, **41f**, 36 ± 4 v.s veh., 38 ± 3.

<u>Tackling solubility.</u> Overall, we had an excellent starting point for further optimization. On the other hand, an improved solubility profile could facilitate the development of this class of

compounds. To tackle this issue, we employed different strategies, such as decreasing the number of aromatic systems[20], replacing phenyl rings with heteroaryls, or introducing polar substituents. In terms of potency, replacing the *N*-benzyl substituent by heterocyclic or acyclic systems was tolerated. Compound **9** (Scheme 1), for instance, was prepared *via* activation of commercially available 2-(2,2,2-trifluoroethoxy)ethan-1-ol and alkylation of 3-nitropyrazole (→ compound **7**), followed by reduction (→ compound **8**) and amide coupling. The synthesis of tetrahydropyrans **15a** and **15b** was more complex. Activation of commercially available (3,4-dihydro-2*H*-pyran-2-yl)methanol, and *N*-alkylation led to compound **10**. Hydroboration (→ compound **11**), *Dess-Martin* oxidation (→ compound **12**), and fluorination led to racemic compound **13** with two fluoro-substituents mimicking the 3,4-difluoro pattern of compound **6j**. Both enantiomers were separated by chiral HPLC. We did not determine their absolute configuration, and classified them arbitrarily as first and second eluting enantiomers. Subsequent reduction to compounds **14a** and **14b**, respectively, and amide couplings led to the desired products.

Compounds **9**, **15a**, and **15b** showed an improved solubility profile, with values in the range of 10 - 20 mg/L in an aqueous buffer at pH 7 (Table 3). However, compound **9** (as many other compounds with an acyclic substituent on the pyrazole) was less potent than our best analogues. Nevertheless, compounds **15a** and **15b** displayed potencies deserving further attention. It should be noted that both enantiomers were equipotent, demonstrating no differentiation with regard to stereochemistry. Unfortunately, aminopyrazole **14b**, a potential metabolite of compound **15b**, was found to be positive in an *Ames* test, which led us to discontinue this subseries (*vide infra*). Also, compound **15a**, while showing reasonable stability in human liver microsomes (CL_{int} = 43 μL/min/mg protein), was metabolically unstable in rat (rat liver microsomes: CL_{int} > 500

μL/min/mg protein; in vivo at 1 mg/kg iv: Cl > 100 mL/min/kg), rendering further evaluations of

this compound difficult.

First enantiomer: **15a**
Second enantiomer: **15b**

First enantiomer: **14a**
Second enantiomer: **14b**

(*rac.*)-**13**
First enantiomer: **13a**
Second enantiomer: **13b**

Scheme 1. (i) MsCl, Et₃N, CH₂Cl₂, 0 °C, 1 h; (ii) 3-Nitropyrazole, NaH, DMF, rt, overnight; (iii) Zn, NH₄Cl, acetone, water, rt, 1 h; (iv) 4-Isopropylphenylacetic acid, EDC·HCl, DMAP, DMF, rt, overnight, 23%; (v) MsCl, Et₃N, CH₂Cl₂, 0 °C, 45 min; (vi) 3-Nitropyrazole, NaH, DMF, rt to 120 °C, 4 h, 76%; (vii) BH₃·THF, THF, 0 °C to rt, 4 h, then 30% H₂O₂/H₂O, 5M aq. NaOH, 0 °C to rt, 2 h, 30%; (viii) Dess-Martin periodinane, NaHCO₃, CH₂Cl₂, rt, overnight, 15% over 2 steps; (ix) Et₃N·3HF, XtalFluor-E®, CH₂Cl₂, rt, 2 h, 93%; (x) Prep. chiral HPLC (column ChiralCel AS-H, heptane:EtOH 1:1); (xi) H₂, Pd/C, EtOAc, rt, 3 h, quant.; (xii) 4-Isopropylphenylacetic acid, EDC·HCl, DMAP, DMF, rt, 3 days, 78-86%.

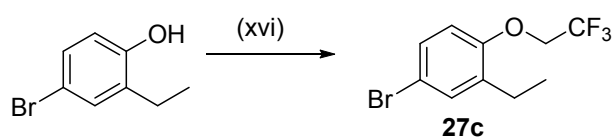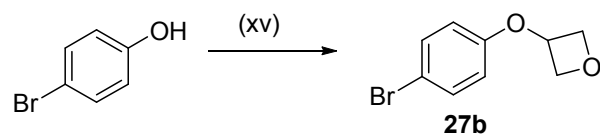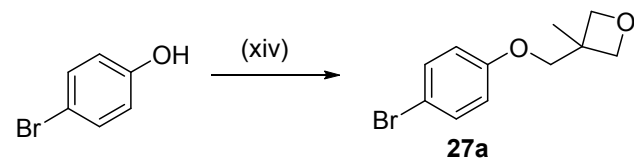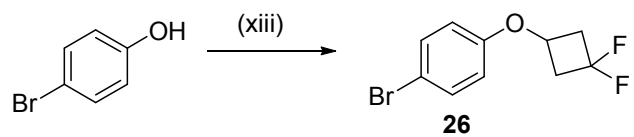**Table 3.** Potency of aminopyrazoles on T-type calcium channels

Compound	Ca$_v$3.1 IC$_{50}$ in nM^a	Ca$_v$3.2 IC$_{50}$ in nM^a	Ca$_v$3.3 IC$_{50}$ in nM^a	Sol. @ pH7 in mg/L
9	14 (6.8-38)	62 (28-180)	3.4 (2.5-4.7)	19
15a	5.6 (1.6-25)	14 (5.9-38)	1.6 (0.4-8.6)	8
15b	2.2 (0.9-5.7)	5.5 (1.7-21)	1.2 (0.6-2.3)	22

^{a}IC$_{50}$ values are the geometric mean of at least three measurements, 95% confidence intervals are indicated in parenthesis. Data were obtained with a Fluorescence Imaging Plate Reader (FLIPR$^®$) assay, see supporting information for detail.

Metabolic stability, solubility, and efflux: optimizing the *para*-position of the phenylacetic acid moiety. At this stage, all compounds containing an *N*-benzyl group, and displaying moderate-to-high solubility in an aqueous buffer at pH7 bore a dimethylaniline moiety at the *para*-position of the phenylacetyl moiety. Metabolic studies on compound **5j** had demonstrated that *N*-demethylation was a major metabolic pathway in human hepatocytes. Since aminophenyl derivatives are known to be potentially mutagenic, the replacement of this dimethylaniline moiety was desirable.

For this reason, we investigated the SAR at the *para*-position of the phenylacetyl moiety thoroughly. In a first step, we maintained the 3-amino-1-(3,4-difluorobenzyl)pyrazole moiety constant. Most compounds were prepared *via* a final amide coupling with the corresponding carboxylic acid. The carboxylic acids themselves, if not commercially available, were prepared in two steps from the corresponding bromophenyl or bromoheteroaryl and 2-*tert*-butoxy-2-oxoethylzinc chloride *via* a *Negishi* coupling (→ compounds of type **17**, Scheme 2), followed by hydrolysis of the *tert*-butyl ester (→ compounds of type **18**). In certain cases, a few additional steps were necessary to prepare the bromo(hetero)aryl derivative. Thus, acid **18b** was prepared from *p*-bromostyrene *via* a [2+2]-cycloaddition (compound **19**) followed by difluorination,

which yielded compound **20**, which in turn was sequentially transformed into ester **17b** and carboxylic acid **18b**. Aminopyridines **21a** and **21b** were obtained by $S_N Ar$ from 2,5-dibromopyridine. Acid **18f** was prepared in one step from the corresponding, commercially available chloropyridine derivative. From the same starting material, an amide coupling led to product **22**, on which the cyclopropyl substituent was introduced leading to the final amide **16g**. A rhodium-catalyzed 1,4-addition yielded the ester **23**, which was reduced to the aldehyde **24**. After decarbonylation, compound **25** was obtained, which was proceeded further through the sequence reported above. Ether **26** was prepared *via* a *Mitsunobu* coupling. Ethers **27a**, **27b**, and **27c** were synthesized by nucleophilic substitution of 4-bromophenol or 4-bromo-2-ethylphenol, respectively, with the corresponding mesylates or triflates.

1
2
3
4
5
6
7
8
9

20, **21a-b**, **25**, **26**, **27a-c**,
or commercially available
starting material

17b-e, 17h-i, 17k-v

18b-e, 18h-i, 18k-v

19

20

21a

21b

18f

22

16g

23

24

25

26

27a

27b

27c
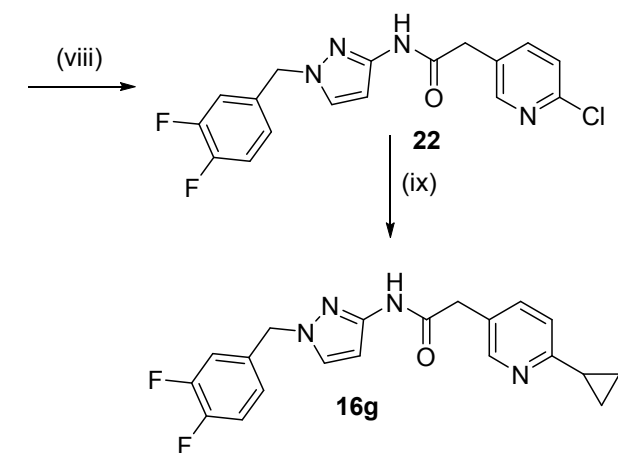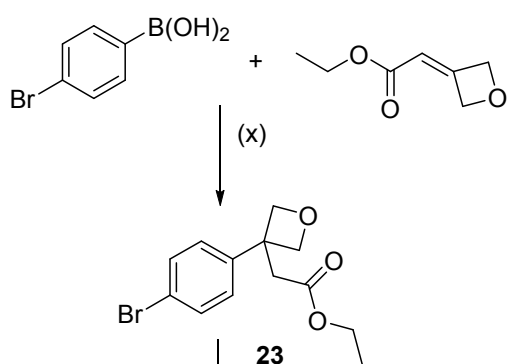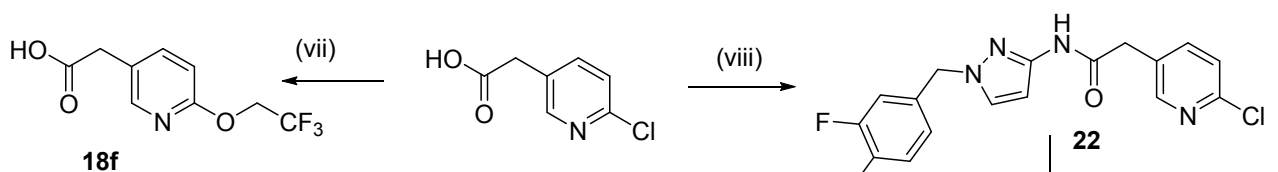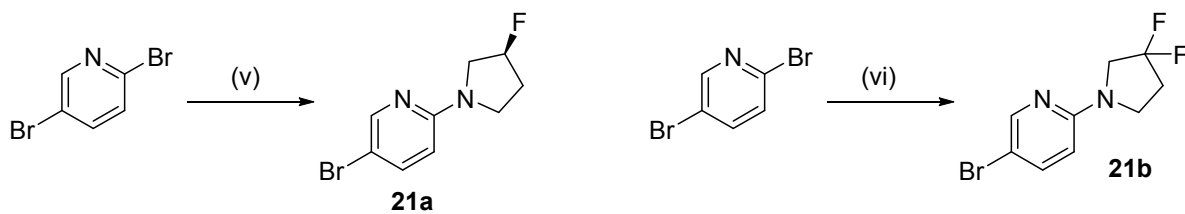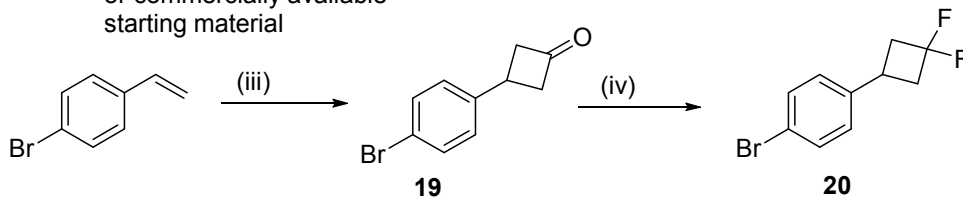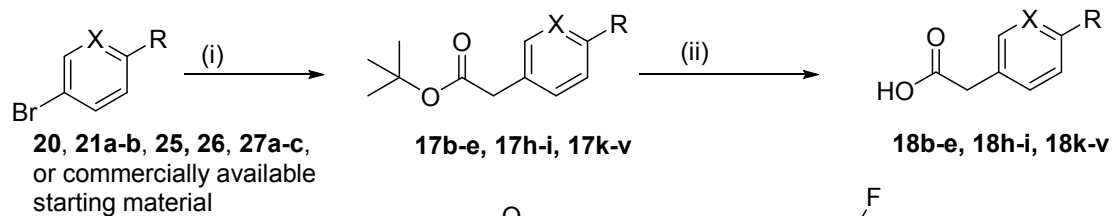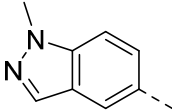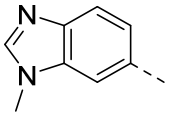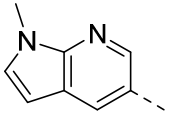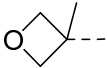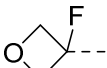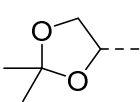
Scheme 2. (i) ClZnCH$_2$CO$_2^t$Bu, Pd-cat., exact conditions see suppl. information; (ii) HCl/dioxane or HCOOH, exact conditions see suppl. information; (iii) DMA, Tf$_2$O, 2,4,6-collidine, CH$_2$ClCH$_2$Cl, 130 – 80 °C, overnight, 42%; (iv) BF$_3$·Et$_2$O, Deoxo-Fluor$^®$, CH$_2$Cl$_2$, toluene, 55-65 °C, 36 h, 30%; (v) (*S*)-3-Fluoropyrrolidine, DBU, DMSO, 90 °C, 7 days, 74%; (vi) 3,3-Difluoropyrrolidine, DBU, DMSO, 80 °C, 1 week, 75%; (vii) NaH, trifluoroethanol, 160 °C, 7 h, quant.; (viii) 1-(3,4-Difluorobenzyl)-1*H*-pyrazol-3-amine, HATU, DIPEA, DMF, rt, overnight, 68%; (ix) Cyclopropylboronic acid, PEPPSI-IPr, K$_3$PO$_4$, toluene, 100 °C, overnight, 11%; (x) [Rh(COD)Cl]$_2$, KOH, dioxane, rt, overnight, 78%; (xi) DIBAL-H, CH$_2$Cl$_2$, -78 °C, 45 min, quant.; (xii) [Rh(COD)Cl]$_2$, DPPP, xylene, 140 °C, 6 h, 56%; (xiii) 3,3-Difluorocyclobutanol, DEAD, PPh$_3$, toluene, 100 °C, overnight, 92%; (xiv) (a) 3-Methyl-3-oxetanemethanol, MsCl, pyridine, CH$_2$Cl$_2$, rt, 4 h, 54% (b) KI, K$_2$CO$_3$, DMF, 130 °C, 2.5 h, quant.; (xv) (a) Oxetan-3-ol, MsCl, Et$_3$N, CH$_2$Cl$_2$, 0 °C, 4.5 h, quant. (b) KO^{t}Bu, Bu$_4$NI, DMF, reflux, 18 h, 53%; (xvi) 2,2,2-Trifluoroethyl trifluoromethylsulfonate, Cs$_2$CO$_3$, DMF, rt, 3 h.

Apolar substituents (Table 4, compounds **16a** and **16b**) led to very potent triple blockers. Not surprisingly, such compounds were only little soluble in an aqueous buffer at pH 7. Replacement of the phenyl group by a pyridinyl led to aminopyridinyl **16c** – **16e**, which were well tolerated in terms of potency. Compounds **16c**, and **16d** were soluble in aqueous buffer, but moderately potent on the Ca$_v$3.2-cha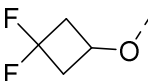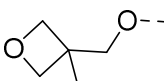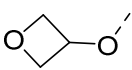nnel; difluoropyrrolidine **16e** increased potency on the Ca$_v$3.2-channel, and led to a simultaneous decrease in solubility at pH7. When combined with the pyridinyl ring, alkoxy substituents (**16f**) or cycloalkyl substituents (**16g**) were less potent. Moving the nitrogen atom of the pyridinyl ring to other positions, as well as the replacement of this heteroaryl with a pyrimidinyl or a five-membered heteroaryl were not tolerated (data not shown). Unfortunately, these aminopyridinyl derivatives tended to be Pgp substrates, as this was the case for compound **16d** (P$_{appA→B}$ = 5.1·10^{-6} cm/s, P$_{appB→A}$ = 61·10^{-6} cm/s, ratio B→A/A→B = 12). The introduction of a lactame (**16h**) or of an oxazolidinone (**16i)** was well tolerated, with a marked increase in solubility for the former example. Unfortunately, here again both compounds were Pgp substrates (**16h**: P$_{appA→B}$ = 3.5·10^{-6} cm/s, P$_{appB→A}$ = 76·10^{-6} cm/s, ratio B→A/A→B = 22; **16i**: P$_{appA→B}$ = 11·10^{-6} cm/s, P$_{appB→A}$ = 59·10^{-6} cm/s, ratio B→A/A→B = 5.5). The introduction of a fused heteroaryl moiety (compounds **16j** – **16n**) was initially not a preferred strategy, since this

increased the global aromaticity of the compounds. Nevertheless, indoles **16j** and **16k** were well tolerated, while the solubilizing effect in aqueous buffer remained somewhat unpredictable. Both compounds penetrated well into the brain when administered to Wistar rats at a dose of 10 mg/kg po (sacrificed at 1 h, **16j**: $C_{total,brain} = 4111 \pm 223$ nM, $C_{CSF} = 50 \pm 11$ nM; **16k**: $C_{total,brain} = 4684 \pm 1701$ nM, $C_{u,brain} = 52 \pm 19$ nM, $C_{CSF} = 164$ nM, single value). Unfortunately, these indoles were chemically unstable, and in their amorphous form degraded within a few days at room temperature. Introducing substituents at positions 1 and 3 led to potent compounds, but chemical stability was not improved (data not shown). The introduction of an indazole (compound **16l**) led to a potent and soluble compound with promising brain penetration (Wistar rats, 10 mg/kg po, sacrificed at 1 h, $C_{u,plasma} = 72 \pm 11$ nM, $C_{u,brain} = 51 \pm 7$ nM, $C_{CSF} = 92 \pm 42$ nM). Unfortunately, a potential metabolite of this compound proved to be positive in an *Ames* test, such that further investigations on compound **16d** were put on hold (*vide infra*). Benzimidazole (compound **16m**) or a pyrrolopyridine derivative (compound **16n**) were found less potent. Since we knew that ethers were generally tolerated (compounds **5e** – **5g**), the SAR was extended to oxetanes (**16o**, **16p**), dioxolane (compound **16q**), and to more complex combination of ethers and oxetanes (compounds **16r-16t**). In general, potency was maintained, and solubility increased at pH7, with the exception of the poorly soluble compound **16r**. Compound **16p** was administered to Wistar rats at 10 mg/kg po and showed good exposure in the brain after 1 h ($C_{total,brain} = 2988 \pm 402$ nM, $C_{u,brain} = 63 \pm 8.4$ nM, $C_{CSF} = 135 \pm 25$ nM). In WAG/Rij rats, oral administration of 10 mg/kg **16p** suppressed completely all seizures for the first 6 h following administration and when looking over the 12 h following administration, it decreased the cumulative duration of seizures by 78% (Fig. 3b).

Table 4. Potency of aminopyrazoles on TTCCs

16a-g, 16o-t   16h-n
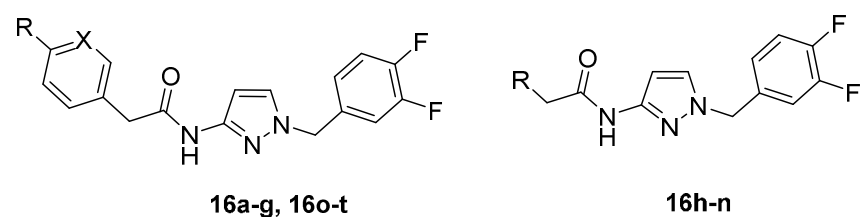
Compound	R	X	Ca$_v$3.1 IC$_{50}$ in nM[a]	Ca$_v$3.2 IC$_{50}$ in nM[a]	Ca$_v$3.3 IC$_{50}$ in nM[a]	Sol. @ pH 7 in mg/L[b]
16a	iPr-	CH	1.4 (1.1-1.7)	6.0 (1.6-29)	1.8 (0.9-3.9)	<1
16b		CH	1.0 (0.5-2.5)	6.1 (5.5-6.7)	1.8 (0.1-63)	-
16c	Me$_2$N-	N	12 (1.0-270)	46 (22-120)	4.0 (2.1-8.6)	25
16d		N	2.5 (1.2-6.2)	21 (11-47)	5.4 (2.2-18)	19
16e		N	1.1 (0.9-1.4)	6.7 (4.2-11)	2.3 (1.2-4.9)	3
16f	CF$_3$CH$_2$O-	N	10 (8.5-12)	140 (16-2200)	11 (4.2-30)	-
16g		N	15 (9.5, 22)	220 (17-6200)	10 (5.6-20)	31
16h		-	1.3 (0.4-5.7)	3.8 (0.3-120)	1.8 (0.7-6.2)	50
16i		-	3.4 (1.7-7.9)	15 (1.2-1700)	2.8 (1.3-7.1)	6
16j		-	1.9 (1.0-3.6)	5.3 (0.5-130)	1.9 (0.8-5.0)	2
16k		-	2.3 (1.4-4.6)	14 (10-20)	2.1 (1.6-2.6)	26

	Structure					
16l		-	3.4 (1.4-4.6)	8.4 (2.8-30)	0.76 (0.4-1.8)	33
16m		-	45 (24-91)	120	9.0 (6.4-13)	-
16n		-	7.1	35	3.3	14
16o		CH	2.4 (1.1-5.3)	4.3 (0.5-64)	1.2 (0.7-2.5)	7
16p		CH	4.3 (2.3-9.6)	13 (5.0-45)	1.3 (0.8-2.1)	25
16q		CH	3.4 (1.8-6.8)	10 (6.0-15)	1.8 (1.2-2.8)	19
16r		CH	1.4 (0.5-4.4)	11 (1.9-110)	6.1 (2.3-18)	<1
16s		CH	3.5 (1.6-8.2)	34 (16-76)	6.6 (4.2-10)	16
16t		CH	4.6 (0.7-54)	32 (18-57)	3.6 (2.0-6.9)	5

[a]IC$_{50}$ values are the geometric mean of at least two measurements. Where sufficient data was available for calculation 95% confidence intervals are indicated in parenthesis. Data were obtained with a Fluorescence Imaging Plate Reader (FLIPR®) assay, see supporting information for detail.

[b]Single measurement

An amide bond hydrolysis leading to an Ames positive metabolite – reoptimization of the N-benzyl moiety. While compounds such as **16l** or **16p** seemed suitable for further profiling, we found that the amide bond of this class of compounds was often slowly hydrolyzed in human and rat plasma. Compound **16k**, for instance, showed a half-life time of 2 h and 5 h in human and rat

plasma, respectively, with the release of 3-amino-*N*-benzylpyrazole **57a** (see Table 9). This metabolite was positive in the *Ames* test, using a bacterial reverse mutation (*vide infra*). A positive *Ames* test does not represent a proof of mutagenicity *per se*, but such a result would require extensive in vitro and in vivo studies to definitely assess the mutagenic potential of such a compound. To facilitate further development it was thus decided that the release of an *Ames* positive aminopyrazole moiety should be preferably prevented. We designed different strategies in order to circumvent this issue: 1. Substitute the α-position of the phenylacetyl moiety to prevent hydrolysis; 2. Develop amide isosteres; 3. Introduce a methylene between the amide and the heteroaryl; 4. Inverse the amide bond; 5. Replace the aminopyrazole moiety by another aminoheteroaryl (pyrazole or other) that would be negative in an *Ames* test. In the following paragraphs, we present the results of these different strategies.

Substituted α-position. Compounds **28a**, and **28b** were prepared *via* amide coupling from commercially available starting material (see supplemental information for details). In general, a short substituent at the α-position was well tolerated (compound **28a**, Table 5, compare with compound **5i**). Unfortunately, this did not stabilize the amide bond against hydrolysis (Table 5). A double substitution generally led to more stable, but much less potent compounds (see compound **28b**). In efforts going into this direction, replacement of the amide bond by a carbamate or a urea led to compounds that were significantly less potent as well (data not shown).

Table 5. Potency of aminopyrazoles on TTCCs

28a   28b
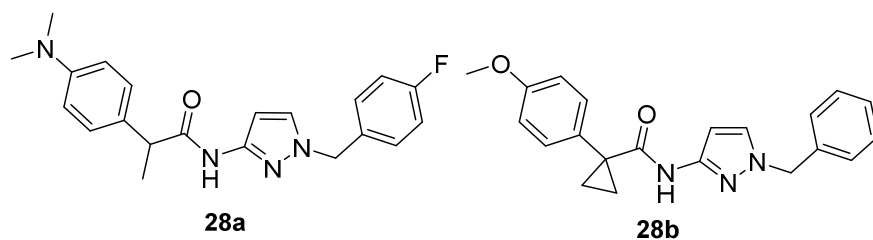
Compound	Ca$_v$3.1 IC$_{50}$ in nM^a	Ca$_v$3.2 IC$_{50}$ in nM^a	Ca$_v$3.3 IC$_{50}$ in nM^a	Percentage hydrolyzed after 6 h in human plasma^b
5i	5.1 (3.7-7.7)	23 (10-91)	7.6 (3.5-26)	4%
28a	6.2 (3.1-13)	44 (14-160)	4.7 (2.5-9.3)	7%
28b	920	2100	1700	<1%

^{a}GIC$_{50}$ values based on single measurements are indicated in italics, other IC$_{50}$ values are the geometric mean of at least three measurements, 95% confidence intervals are indicated in parenthesis. Data were obtained with a Fluorescence Imaging Plate Reader (FLIPR$^®$) assay, see supporting information for detail.

^{b}Single measurement

Amide isosteres. Replacing the carboxamide with an isostere is an obvious way to prevent any release of an aminoheteroaryl metabolite. Therefore, we synthesized five-membered heteroaryls as amide isosteres, a few of which are exemplified hereafter (Scheme 3). A fused system like a pyrazoloimidazole was built mainly following known literature procedures[21], leading to compound **32a**. Five-membered heteroaryl, either preserving a benzylic position, like triazole **32b**, or with the terminal phenyl ring directly linked to the isosteric ring, like oxadiazole **32c**, were prepared as well, using standard procedures *via* intermediates **33**, **34**, and **35**. Unfortunately, as depicted in Table 6, all these analogues led to substantial losses in biological activity. While the fused system **32a** maintained potencies about ten-fold lower than its amide analogue **6e**, compound **32b** was in the high nanomolar range, and compound **32c** was completely inactive.

29

30

31

32a

33

34

32b

35

32c
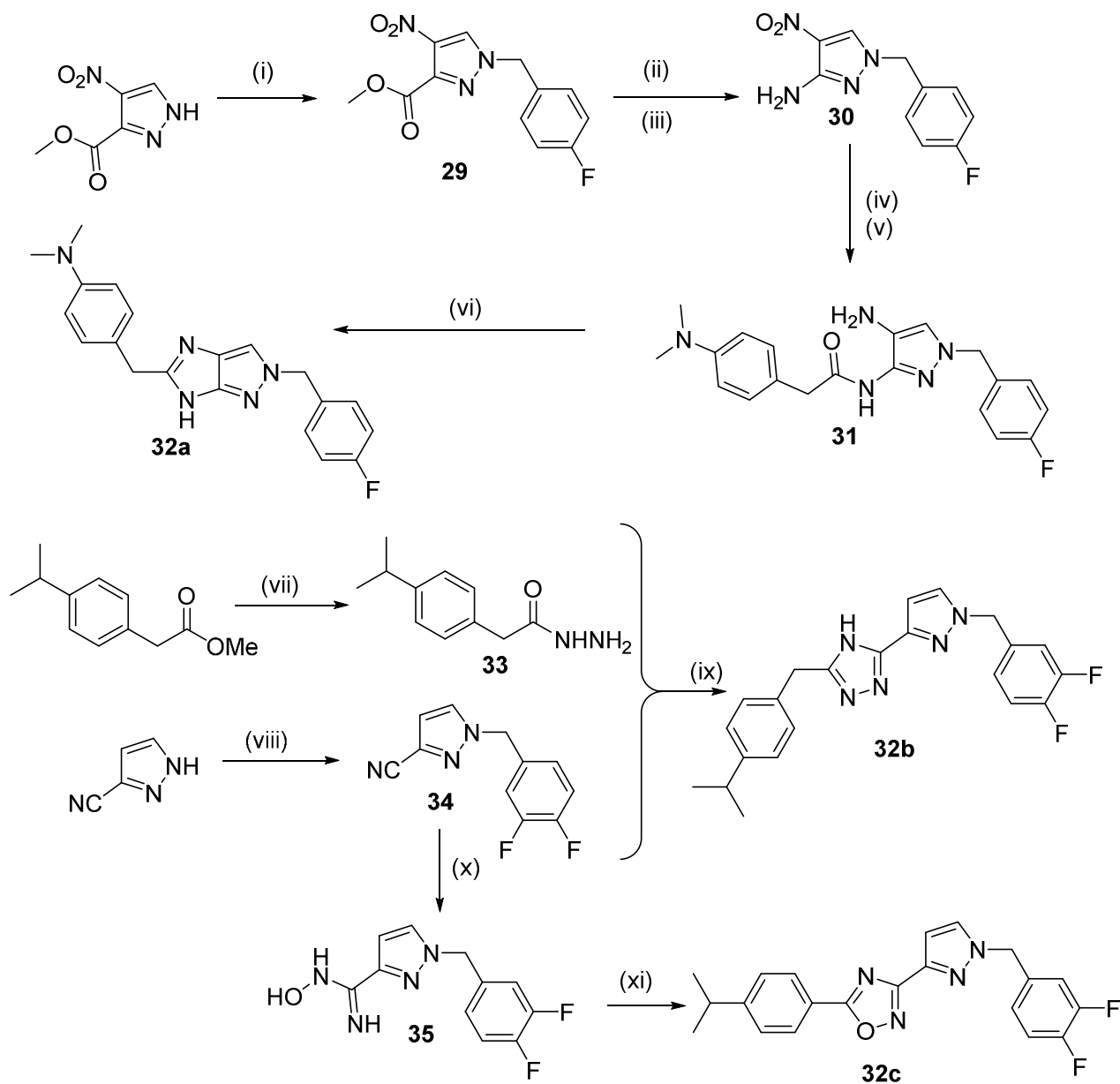
Scheme 3. (i) K$_2$CO$_3$, 4-fluorobenzyl bromide, CH$_3$CN, rt, overnight, 69%; (ii) Aq. 2.5M NaOH, MeOH, reflux, 1 h, 93%; (iii) DPPA, Et$_3$N, ^{t}BuOH reflux, 1 h, then TFA, CH$_2$Cl$_2$, rt, 2 days, 87%; (iv) H$_2$, Pd/C, HCl, H$_2$O, MeOH, rt, 3 h, 37%; (v) 4-(Dimethylamino)phenylacetic acid, HATU, DIPEA, DMF, rt, 1 h; (vi) POCl$_3$, reflux, 7.5 h, 12% over two steps; (vii) H$_2$NNH$_2$·H$_2$O, 90 °C, 2 h, 88%; (viii) 3,4-Difluorobenzyl bromide, Cs$_2$CO$_3$, DMF, rt, overnight, 75%; (ix) K$_2$CO$_3$, n-BuOH, reflux, 2 days, 1%; (x) H$_2$NOH·HCl, EtONa, EtOH, reflux, overnight, 63%; (xi) 4-Isopropylbenzoyl chloride, pyridine, toluene, reflux, overnight, 23%.

Table 6. Potencies on TTCCs

Compound	$Ca_v3.1$ IC_{50} in nM[a]	$Ca_v3.2$ IC_{50} in nM[a]	$Ca_v3.3$ IC_{50} in nM[a]
32a	60 (20-240)	160 (68-420)	10 (6.0-16)
32b	*180*	*260*	*420*
32c	*>10000*	*>10000*	*>10000*
39a	55 (21-160)	160 (37-1000)	8.0 (5.4-12)
39b	22 (3.8-200)	140 (32-810)	9.8 (4.7-21)

[a]IC_{50} values based on single measurements are indicated in italics, other IC_{50} values are the geometric mean of at least three measurements, 95% confidence intervals are indicated in parenthesis. Data were obtained with a Fluorescence Imaging Plate Reader (FLIPR®) assay, see supporting information for detail.

3-Aminomethylpyrazoles. We prepared 3-(aminomethyl)pyrazoles and 3-(1-aminoethyl)-1*H*-pyrazoles (Scheme 4). A double benzylation using commercially available starting materials led to ester **36**, which was reduced to alcohol **37**. Introduction of the amine *via* phthalimide **38**, and subsequent amide coupling led to compound **39a**. Aminoethyl derivative **39b** was prepared *via* aldehyde **40**, which was then subjected to *Ellman*'s sulfinamide procedure[22]. Unfortunately, these derivatives were at least ten times less potent on the $Ca_v3.2$ channel (Table 6) than the corresponding 3-aminopyrazole analogue (compound **16a)**. Despite the extensive SAR studies, including the preparation of benzamide analogues, we were not able to obtain potent TTCC blockers in this subseries.
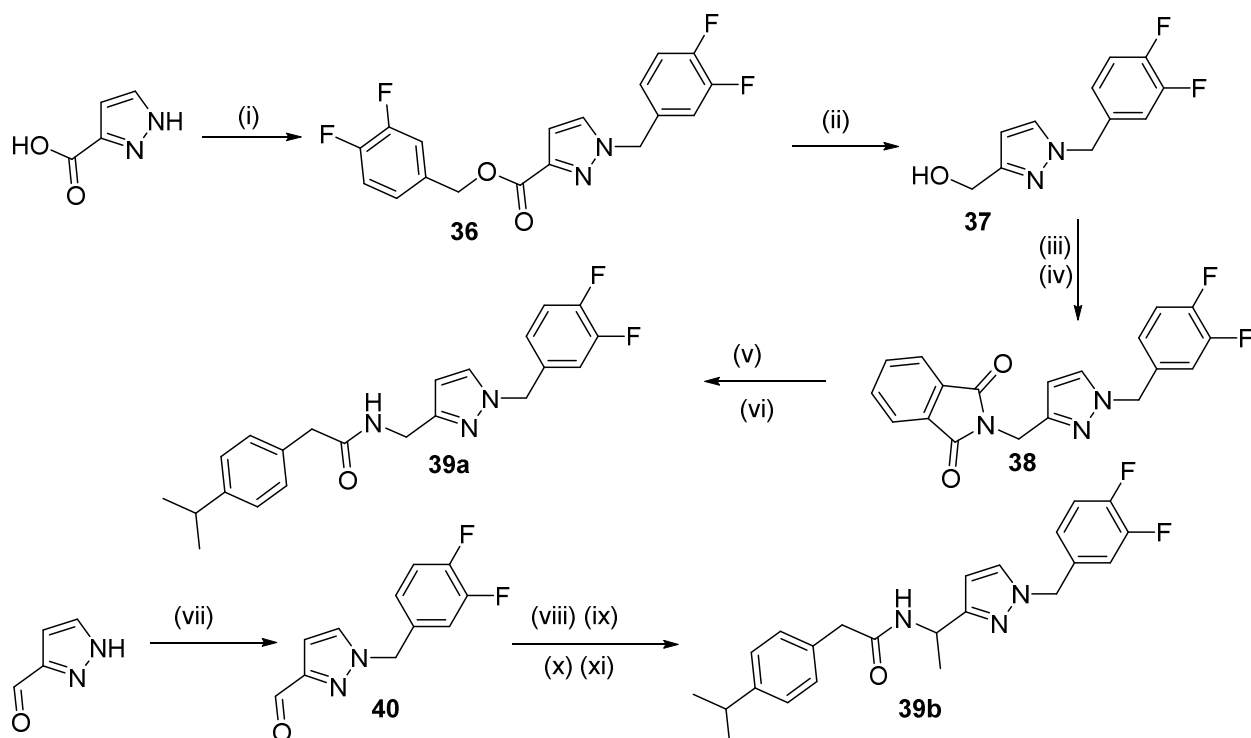
Scheme 4. (i) 3,4-Difluorobenzyl bromide, Cs_2CO_3, DMF, rt, overnight, 52%; (ii) $LiAlH_4$, THF, 0 °C to rt, 2 h, 78%; (iii) PBr_3, toluene, reflux, 15 min; (iv) Cs_2CO_3, phthalimide, DMF, rt, overnight, 75% over two steps; (v) $H_2NNH_2 \cdot H_2O$, EtOH, rt, 3 h; (vi) 2-(4-Isopropylphenyl)acetic acid, EDC·HCl, DMAP, DMF, rt, overnight, 88% over two steps; (vii) 3,4-Difluorobenzyl bromide Cs_2O_3, DMF, rt, overnight, 67%; (viii) 2-Methyl-2-propanesulfinamide, $Ti(OEt)_4$, THF, rt, overnight; (ix) MeMgBr, THF, 0 °C to rt, 17 h; (x) HCl, dioxane, MeOH; (xi) 4-Isopropylphenylacetic acid, TBTU, DIPEA, DMF, rt, 30 min, 50% over 4 steps.

Inverse amides. An inverse amide would, in case of hydrolysis, lead to a pyrazole carboxylic acid, and to a benzylic amine, which are both not expected to be *Ames* positive. To give a few examples from the numerous compounds we prepared following this strategy, compounds **41a** – **41d** were prepared as described in Scheme 5. Carboxylic acid **43** was prepared by *N*-alkylation of methyl 1*H*-pyrazole-3-carboxylate (compound **42**) and subsequent saponification. Standard amide coupling procedures with commercially available amines yielded products **41a** and **41b**. Alkylation of oxetan-3-one led to alcohol derivative **44**, which was fluorinated to compound **45**. Deprotection led to amine **46**, which was coupled to acid **43** to yield amide **41c**. Eventually, a

S_NAr led to nitrile **47**, and subsequent reduction to amine **48**. An amide coupling with acid **43**

delivered product **41d**.
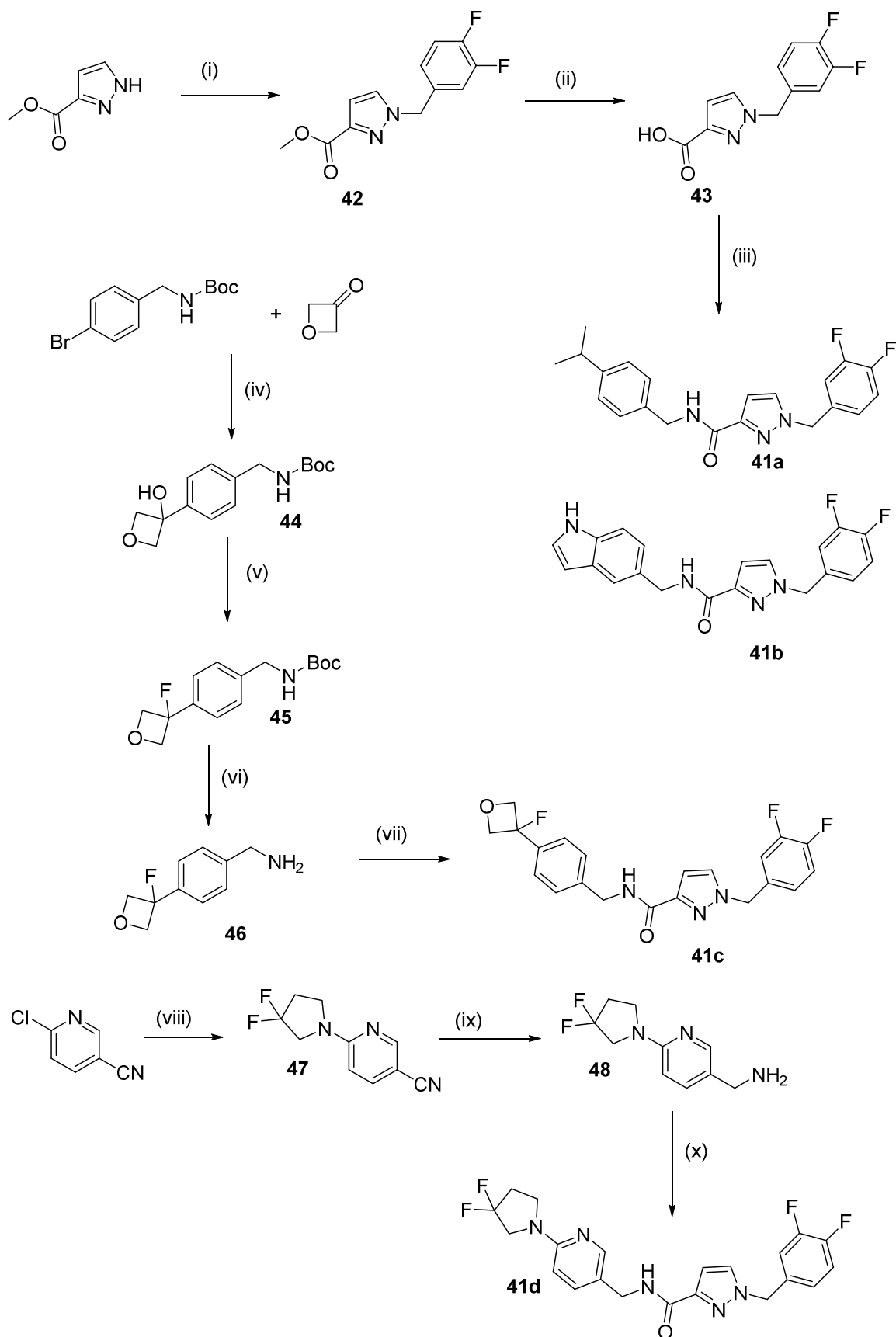
Scheme 5. (i) 3,4-Difluorobenzyl bromide, Cs_2CO_3, DMF, 60 °C, 1 h, 52%; (ii) NaOH, MeOH, H_2O, rt, 3 h, 98%; (iii) (a) $(COCl)_2$, toluene, rt, 1 h; (b) (4-Isopropylphenyl)methanamine, CH_2Cl_2, rt, overnight, 37%; (iv) MeMgCl, *n*-BuLi, 3-oxetanone, THF, -78 °C to rt, 6 h, 46%; (v) DAST, CH_2Cl_2, -78 °C to rt, 2 h, 49%; (vi) HCOOH, rt, 2 h, 93%; (vii) HATU, DIPEA, DMF, rt, 1 h, 16%; (viii) 3,3-Difluoropyrrolidine hydrochloride, DIPEA, DMF, 85 °C, 22 h, 97%; (ix) Ra-Ni, H_2, 50 bar, NH_3, MeOH, 60 °C, 5 h, quant.; (x) DMAP, EDC·HCl, DMF, rt, 6 h, 67%.

Other heterocyclic systems replacing the pyrazole moiety were prepared as well (Scheme 6).

Ethyl 2*H*-1,2,3-triazole-4-carboxylate was benzylated to derivative **49** (regioselectivity 2:1 in

favor of compound **49**), which was saponified to carboxylic acid **50**. A *Negishi* coupling from

ethyl 2-bromooxazole-4-carboxylate and *p*-trifluoromethoxybenzyl bromide led to oxazole **51**,

which was saponified to its corresponding acid **52**. A similar strategy was applied to obtain the

thiazole **54**, *via* intermediate **53**, and to prepare thiazole **56**, from intermediate **55**. Carboxylic

acids **50**, **52**, **54**, and **56**, were subjected to amide couplings to yield the final products **41e**, **41f**,

41g, and **41h** respectively (Table 7).
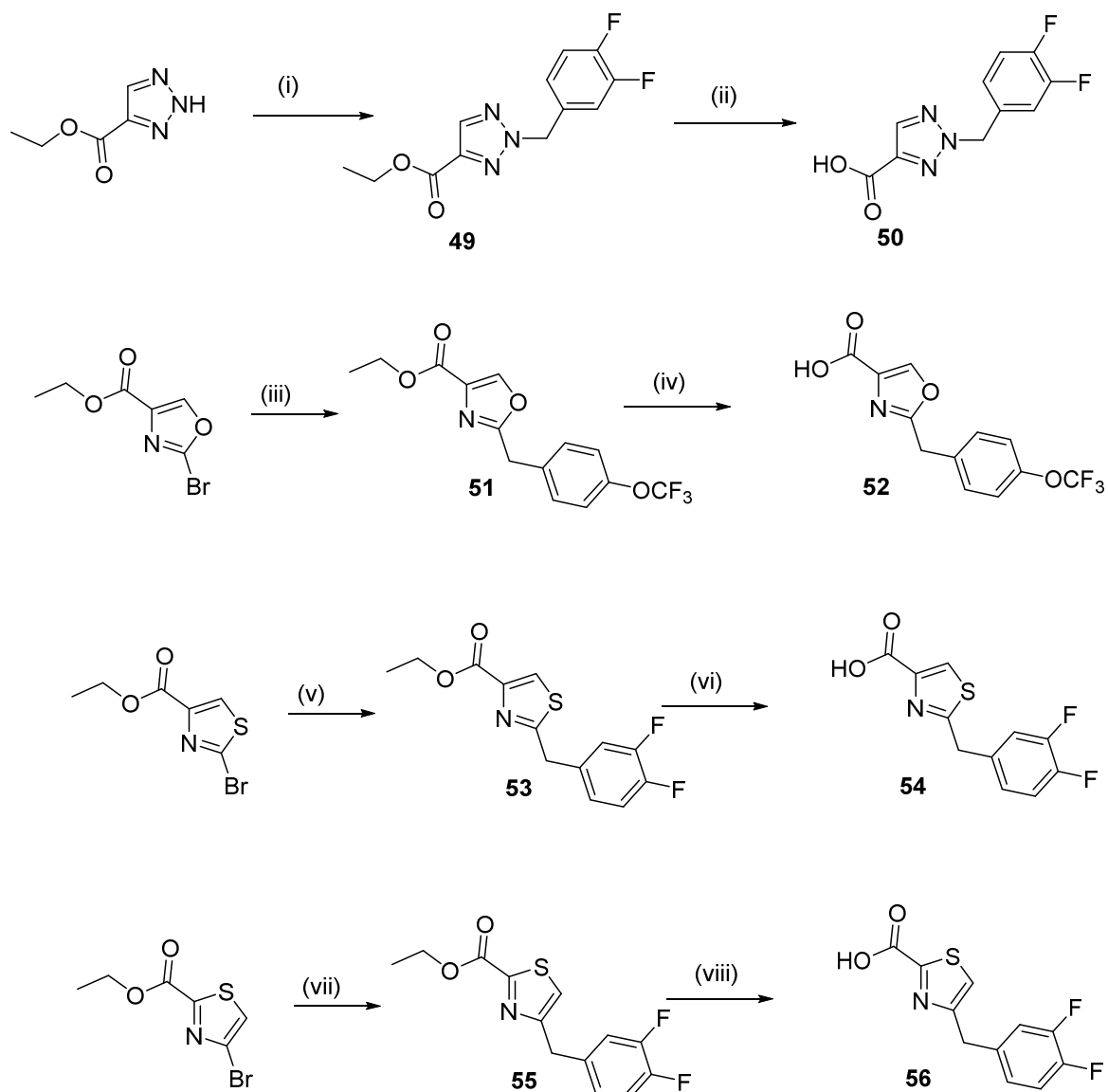
Scheme 6. (i) 3,4-Difluorobenzyl bromide, K_2CO_3, DMF, rt, 1 h, 29%; (ii) Aq. 2.5M NaOH, EtOH, rt, 1 h, 80%; (iii) 4-(Trifluoromethoxy)benzyl bromide, activated Zn, Pd(^{t}Bu$_3$P)$_2$, THF, rt, 5 h; (iv) Aq. 2M NaOH, DMF, rt, overnight, 20% over two steps; (v) 3,4-Difluorobenzyl bromide, activated Zn, Pd(PPh$_3$)$_4$, THF, rt, overnight; (vi) Aq. 2M NaOH, EtOH, THF, rt, 2 h; (vii) 3,4-Difluorobenzyl bromide, activated Zn, Pd(^{t}Bu$_3$P)$_2$, THF, rt, 2 h, 23%; (viii) Aq. 2M NaOH, DMF, rt, 18 h, 76%.

Pyrazoles **41a**, **41b**, **41c**, and **41d** are the exact analogues to pyrazoles **16a**, **16k**, **16p**, and **16e**, respectively. These compounds did not achieve the same potencies as their corresponding analogues (Table 7) and, despite extensive optimization efforts, we were never able to reach this

goal. Investigation of other five-membered heteroaryls (compounds **41e** – **41h**) did not yield very potent compounds either. Nevertheless, compounds **41d** and **41f** were studied further (Table 8). Metabolic stability was in an acceptable range, and aqueous solubility and unbound fraction remained low. This translated into low levels of unbound brain- and plasma concentrations, in spite of good permeability and no active transport by the Pgp pump (**41d**: $P_{appB \rightarrow A} = 53 \cdot 10^{-6}$ cm/s, ratio B→A/A→B = 2.8; **41f**: $P_{appB \rightarrow A} = 15 \cdot 10^{-6}$ cm/s, ratio B→A/A→B = 1.3). In parallel with those data, over the 12 h following oral administration in WAG/Rij rats, 10 mg/kg of **41d** or **41f** did not decrease the cumulative duration of seizure (Figure 3c and d) to a similar extend as compound **6j** and **16p**. Over the 6 h following administration, modest but significant decreases of 32% and 31% were observed for **41d** and **41f** respectively ($p < 0.05$ compared to vehicle treated rats for both compounds, paired t-test). Besides these disappointing results, we confirmed that carboxylic acid **52** was negative in an *Ames* test.

Table 7. Potency of aminopyrazoles on TTCCs
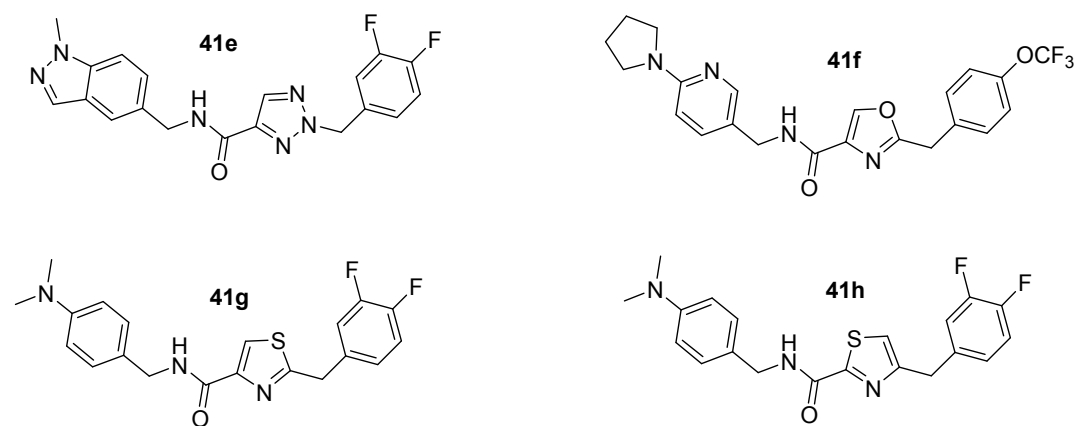
Compound	$Ca_v3.1$ IC_{50} in nM[a]	$Ca_v3.2$ IC_{50} in nM[a]	$Ca_v3.3$ IC_{50} in nM[a]
41a	24 (8.0-84)	74 (11-760)	40
41b	70 (26-210)	330 (180-760)	22 (5.4-120)

41c	53 (17-200)	100 (25-540)	17 (1.6-400)
41d	6.5 (2.8-20)	30 (16-67)	10 (3.9-40)
41e	34 (21-57)	90	14 (4.2-59)
41f	18 (10-33)	30 (16-58)	5.2 (1.2-29)
41g	45 (27-76)	100 (38-330)	15 (10-22)
41h	17 (6.1-58)	71 (21-300)	9.7 (7.0-13)

[a]IC_{50} values are the geometric mean of at least two measurements, where sufficient data is available for calculation 95% confidence intervals are indicated in parenthesis. Data were obtained with a Fluorescence Imaging Plate Reader (FLIPR®) assay, see supporting information for detail.

Table 8. Profile of compounds **41d** and **41f**

Compound	CL_{int} HLM in µL/min/mg protein	Sol. @ pH7 in mg/L	$f_{u,plasma}$	$C_{u,plasma}$[a] in nM	$C_{u,brain}$[a] in nM
41d	87	8	0.007	14 ± 3	5.4 ± 1.2
41f	54	<1	<0.001	<1.2 ± 0.3	4.4 ± 1.4

[a]In Wistar rats, po, 10 mg/kg, sacrifice after 1 h (mean ± SD; n = 3)

Replacement of the aminopyrazole moiety by another aminoheteroaryl that is Ames negative. The positive outcome of a 3-aminopyrazole in the *Ames* test was not a complete surprise, as similar findings can be found in the literature[23]. On the other hand, some aminopyrazoles, like emicerfont (GW876008)[24], have been in clinical development. Genotoxicity of aromatic amines depends upon their potential to be oxidized to the corresponding hydroxylamines, with subsequent acetylation or sulfonation. Resulting acetoxyamines can be cleaved to the nitrenium cation, that in turn alkylates the DNA, in particular at the C(8)-position of deoxyguanosine[25]. Due to this complex mechanism, it is notably difficult to correctly predict their potential mutagenicity and outcome in an *Ames* test. Recently, an attempt to predict the mutagenicity of 5-

aminopyrazoles in an *Ames* test was published[26], and the propensity of aromatic amines to be positive in an *Ames* test has been correlated with the HOMO energy as a propensity for *N*-oxidation[27], or with the formation energy of the nitrenium cation[28], and should be independent of the size of the molecule[28c]. The conflicting results that can sometimes be observed when comparing studies may arise from different data sets, as demonstrated by McCarren *et al.*[28b], but in our opinion may arise as well from different ways of defining *Ames* positive and *Ames* negative results, and from different purities of the tested materials.

Existing prediction tools like Derek Nexus® or Leadscope Model Applier®, may give general trends for the mutagenic potential of aromatic amines in an *Ames* test, but they are not precise enough to predict the outcome of aminopyrazoles and similar structures with fine differences in their substitution patterns. Consequently, we prepared numerous aminoheteroaryls to be evaluated in the *Ames* test on *Salmonella typhimurium* strains TA98 and TA100, with metabolic activation using phenobarbital/beta-naphthoflavone induced rat liver S9-fraction. Under these conditions, several aromatic amines appear positive in this test.[27, 29] A test item was considered positive if a biologically relevant increase in the number of revertants exceeded the threshold by two fold compared to the corresponding solvent controls in any incubation. We had initially compared the standard *Ames* test with the so-called mini-*Ames* or *Ames* II assay[30] but the latter was abandoned as it was unreliable and underestimated the values obtained later on in the standard *Ames* test. Therefore, the compounds were screened in a standard *Ames* format on TA98- and TA100 in the presence of metabolic activation. As mentioned earlier, 3-amino-1-(3,4-difluorobenzyl)pyrazoles **57a** and the tetrahydropyran derivative **14b** were shown to be *Ames* positive (Table 9). Astonishingly, pyrazole **14a**, the enantiomer of pyrazole **14b**, was negative. Nevertheless, concerns about enantiomeric purity in a chemical process led to its abandonment.

From our SAR, we learned that the presence of a heteroatom, preferentially a nitrogen atom, between both exit vectors on the central five-membered heteroaryl, was essential for potency on TTCCs. By introducing a third nitrogen atom, we hoped to reduce the metabolic activation, and we prepared 1,2,3- and 1,2,4-triazoles. 1,2,3-Triazole **57b** was prepared by *N*-alkylation of 4,5-dibromotriazole (→ triazole **58**, Scheme 7), followed by desymmetrization *via* debromination (compound **59**), and subsequent *Ullman* reaction[31]. Triazole **57c** was prepared from 1-(3,4-difluorobenzyl)-3-nitro-1*H*-1,2,4-triazole, by alkylation (→ compound **60**) and subsequent reduction.

1,2,3-Triazoles were promising in terms of potency but, compared to the pyrazole template, they tended to be less tolerant to possible substituents at the *para*-position of the phenylacetyl moiety. Nevertheless, as exemplified by compound **63a** (Table 10), the approach was promising, with high potencies and brain concentrations well above the IC_{50}-values when administered *po* to rats at a dose of 10 mg/kg. Unfortunately, the amino heteroaryl moiety of this compound proved to be *Ames* positive as well (compound **57b**, Table 9). Indeed, we could not identify a TTCC blocker with a 4-amino-1,2,3-triazole scaffold that was both, highly potent and *Ames* negative. The triazole series and the pyrazole series followed very similar trends in terms of sensitivity to the *Ames* test and, to overcome this issue, more polarity needed to be added onto the *N*-benzyl substituent; unfortunately, this led to a marked loss in potency for the triazole series.
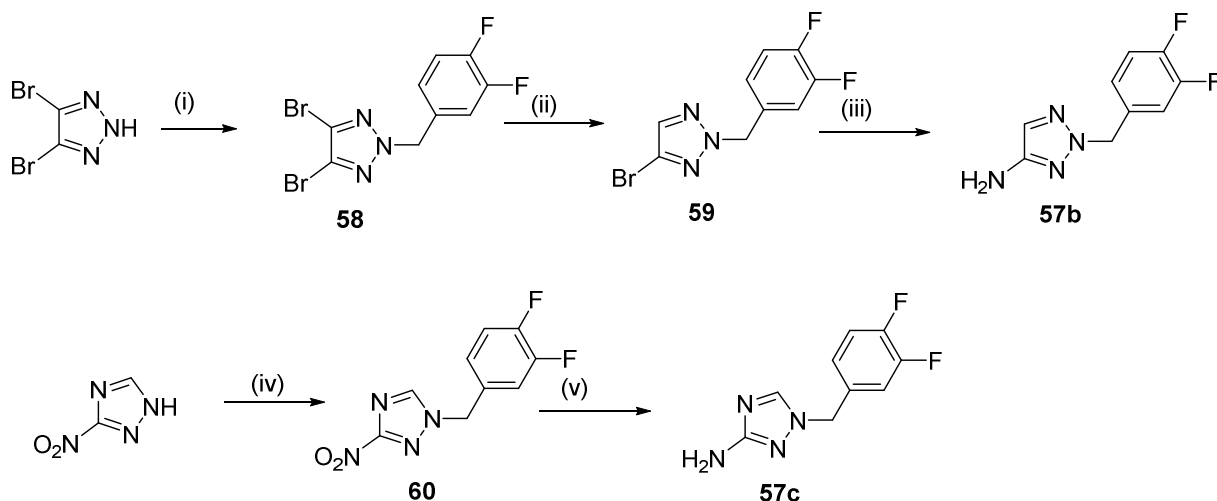
Scheme 7. (i) 3,4-Difluorobenzyl bromide, K₂CO₃, DMF, rt, 1 h, 64%; (ii) *i*PrMgCl, THF, -5 °C to 35 °C, 1 h, 59%; (iii) Aq. 25% NH₃, Cu, 110 °C, 13 days, 76%; (iv) 3,4-Difluorobenzyl bromide, K₂CO₃, DMF, rt, overnight, 81%; (v) Zn, aq. NH₃, acetone, rt, 30 min, quant.

1,2,4-Triazole **57c** on the other hand was negative in an *Ames* test. In order to maintain a reasonable potency in this series, a lipophilic substituent at the phenylacetyl moiety was mandatory: Compound **63b**, for instance, was a potent TTCC blocker. However, not unexpectedly such a lipophilic compound was poorly soluble and consequently had poor exposure leading to unbound brain concentrations below the IC$_{50}$-values (Table 10).

Beyond triazoles, another five-membered heteroaryl that led to potent TTCC blockers was the 2-aminothiazole **57d**. This aminothiazole was prepared by cyclization from bromoketone **62**, which was itself prepared in two steps from 3,4-difluorophenylacetic acid, *via* the diazo derivative **61** (Scheme 8). Its derivative, compound **63c**, was a potent triple blocker, but had low solubility. Furthermore, compound **57d** was *Ames* positive (Table 9).
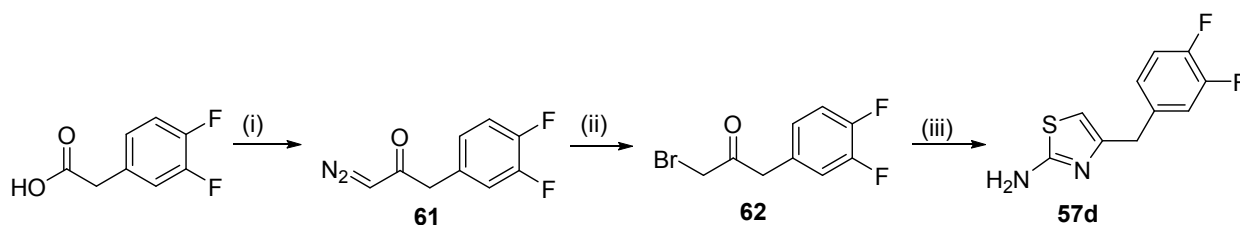
Scheme 8. (i) (a) $(COCl)_2$, DMF, CH_2Cl_2, -5 °C to rt, 2 h, (b) $TMSCHN_2$, THF, -5 °C to rt, overnight, 47%; (ii) HBr, H_2O, AcOH, 0 °C to rt, 2 h, 86%; (iii) H_2NCSNH_2, $NaHCO_3$, EtOH, reflux, 2 h, 94%.

We then returned to the pyrazole template and attempted to decrease the electron density by introducing an electrowithdrawing (and polar) substituent at position 4. Aminopyrazole **57e** was prepared by direct *N*-alkylation of 3-amino-1*H*-pyrazole-4-carbonitrile with 3,4-difluorobenzyl bromide. Aminopyrazole **57e** was *Ames* negative and the introduced 4-nitrile substituent was well tolerated. However, this substituent did not increase solubility; thus, we tried to introduce additional polarity at the phenylacetyl moiety. As exemplified with compound **63d** (Table 10), these compounds remained poorly soluble in aqueous medium at pH7. Unfortunately, this pattern led to active efflux by the Pgp-pump (in MDR1-MDCK cells $P_{appA \rightarrow B} = 1.3 \cdot 10^{-6}$ cm/s, $P_{appB \rightarrow A} = 65 \cdot 10^{-6}$ cm/s, ratio B→A/A→B = 50); active efflux was a hallmark for all 4-cyanopyrazole derivatives, and we had to abandon this sub-series.

Finally, we screened various 3-amino-1-benzylpyrazoles in the *Ames* test. We modulated the benzyl moiety, remote from the presumed site of action at the amino group, postulating that such modifications could influence the compound metabolism. These aminopyrazoles were prepared by *N*-alkylation of 3-nitropyrazole with the corresponding benzyl bromide or chloride, and subsequent reduction of the nitro group (see supporting information for details). In these cases, we paid a particular attention not to detect any residual nitropyrazole. We monitored the purity of our compounds by LC-MS (<0.2%), and tested them only when no organic impurity appeared by ^{1}H-NMR, in particular with regard to residual nitropyrazoles and the isomeric 2-amino-1-

benzylpyrazoles; commercial compounds were recrystallized or purified by preparative HPLC. Having many compounds near the two-fold increase threshold, and taking into account biological variability and non-linearity of the *Ames* test, we were not surprised that this SAR was complex and apparently unpredictable. While an unsubstituted benzyl group (compound **57f**) led to a strong fold increase in the *Ames* test, the introduction of a *para*-fluoro substituent reduced but did not eliminate this signal. Since a *para*-substituent was essential for high potency of the parent compounds on the targets, we focused our efforts on this position. We did not observe a correlation between the fold increase in bacterial strains in the *Ames* test, and position or number of substituents. Electrodonating (e.g. compound **57i**) or neutral (e.g. compound **57h**) groups were more prone to lead to *Ames* positive aminopyrazoles than electrowithdrawing substituents (e.g. compound **57g**). A polar *para*-cyano group (compound **57j**) led to an *Ames* negative aminopyrazole. The corresponding pyridinyl derivative **57k** was *Ames* negative as well. The sensitivity of the substitution pattern is exemplified with compounds **57l** and **57m**, where the simple exchange of fluoro and cyano substituents led to different outcomes. The introduction of a pyridinyl ring on compound **57n** led to an *Ames* negative derivative.

Table 9. Ames results on aminoheteroaryl derivatives
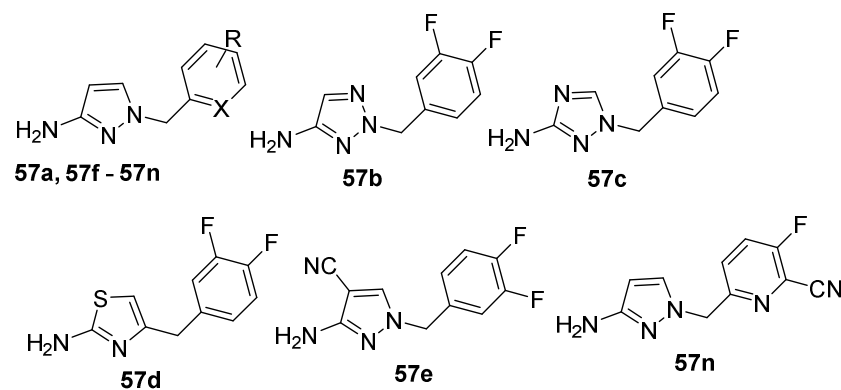
Compound	X	R	TA98 + S9	TA100 + S9

			Fold increase	Fold increase
14a	-	-	1.4	1.3
14b	-	-	1.1	2.5
57a	CH	3,4-di-F	2.7	1.2
57b	-	-	1.3	3.3
57c	-	-	1.1	1.1
57d	-	-	2.7	1.1
57e	-	-	1.1	1.1
57f	CH	H	15.3	30.3
57g	CH	*p*-F	4.1	10.2
57h	CH	*p*-Me	15.1	19.8
57i	CH	*p*-MeO	8.0	20.8
57j	CH	*p*-CN	1.5	1.1
57k	N	*p*-CN	1.0	1.3
57l	CH	*m*-F-*p*-CN	1.2	2.2
57m	CH	*p*-F-*m*-CN	1.5	1.5
57n	-	-	1.2	1.4

Table 10. Triazoles, thiazoles, and cyanopyrazoles
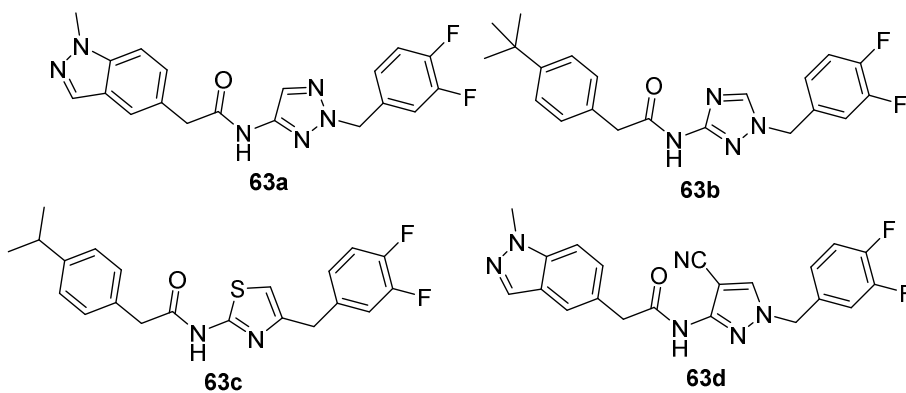
Compound	Ca$_v$3.1	Ca$_v$3.2	Ca$_v$3.3	Sol. @ pH 7	$f_{u,hplasma}$	$C_{u,brain}$

	IC_{50} in nM^a	IC_{50} in nM^a	IC_{50} in nM^a	mg/L^b		nM^c
63a	3.5 (2.2-6.0)	8.6 (4.0-24)	1.5 (0.8-3.5)	<1	0.022	63 ± 14
63b	5.0 (3.2-8.4)	31 (17-61)	7.9 (1.7-95)	2	0.008	2.4 ± 0.3
63c	4.5 (2.1-10)	22 (3.6-220)	7.1 (2.0-31)	<1	<0.001	-
63d	17 (9.5-32)	21 (9.2-53)	10 (4.1-31)	3	0.045	-

^{a}IC_{50} values are the geometric mean of at least three measurements, 95% confidence intervals are indicated in parenthesis. Data were obtained with a Fluorescence Imaging Plate Reader (FLIPR$^®$) assay, see supporting information for detail.

^{b}Single measurement

^{c}In Wistar rats, po, 10 mg/kg, sacrifice after 1 h (mean $\pm$ SD, n = 3)

Final optimization. With these results in hand, we focused our efforts on aminopyrazole **57k** because this compound was *Ames* negative, and the corresponding final products had favorable physicochemical properties leading to soluble final products. Optimization of the phenylacetyl moiety showed that little supplemental polarity would be tolerated; with too much polarity, the final compound became a Pgp substrate. From previous knowledge (Tables 1 and 4), we knew that an apolar group, or possibly a moderately polar ether substituent, could be accommodated at the 4-position of the phenylacetyl moiety. During this final optimization, our attention focused on six compounds (Table 11). Amides **66a**, **66b**, **66e**, and **66f** were prepared following procedures described earlier in this work (see supporting information for details). The carboxylic acid moieties of amides **66c** and **66d** were prepared from methyl 2-(4-hydroxy-3-methylphenyl)acetate and the corresponding electrophile to yield products **64a** and **64b**, respectively, which were saponified to carboxylic acids **65a** and **65b** (Scheme 9).
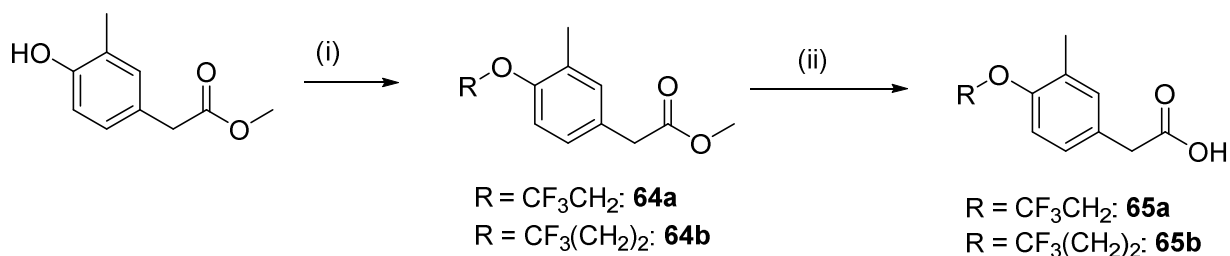
Scheme 9. (i) R-OTs, Cs$_2$CO$_3$, DMF, rt, 20 – 72 h; (ii) Aq. 1M NaOH, THF, rt, 4 h.

Table 11. Final pyrazoles
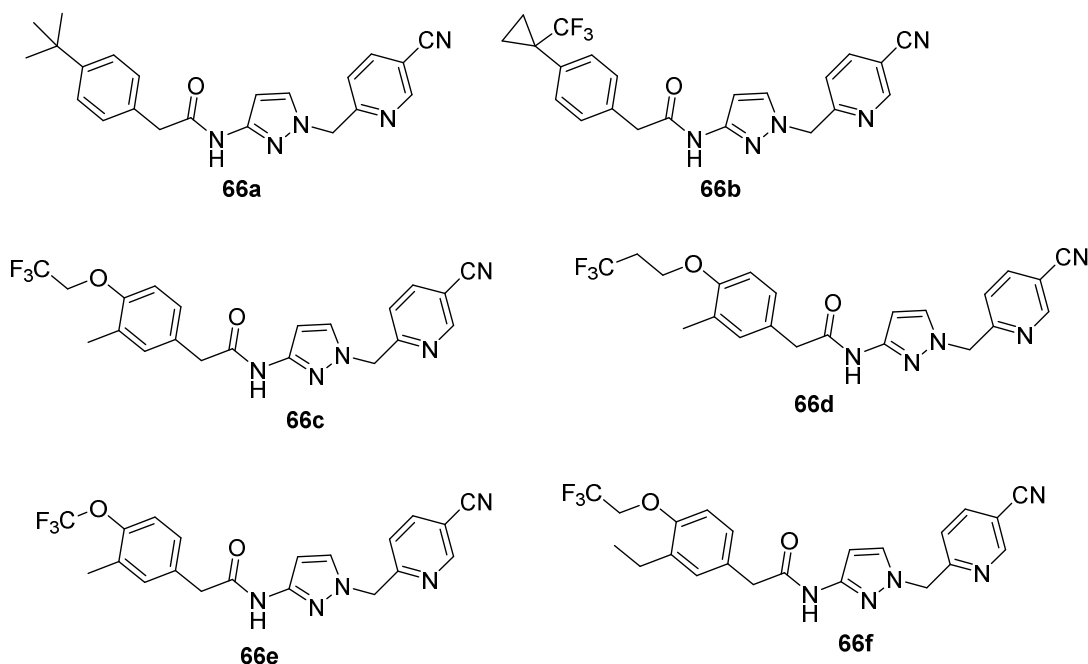
Compound	Ca$_v$3.1 IC$_{50}$ in nM[a]	Ca$_v$3.2 IC$_{50}$ in nM[a]	Ca$_v$3.3 IC$_{50}$ in nM[a]	Ca$_v$1.2 IC$_{50}$ in nM[a]	Sol. @ pH 7 in mg/L[b]	C$_{u,brain}$ in nM[c]
66a	2.8 (2.1-4.0)	7.5 (4.2-17)	2.6 (1.6-4.5)	*2420*	<1	6.1 ± 1.6
66b	6.4 (5.8-11)	18 (16-52)	7.5 (5.4-10)	*2410*	5	29 ± 11
66c	2.2 (0.9-11)	7.0 (5.1-10)	1.7 (1.3-2.2)	*3310*	25	42 ± 2.4
66d	2.6 (1.4-6.0)	18 (12-27)	4.1 (2.2-9.5)	*2080*	12	18 ± 4.8
66e	2.3 (1.8-3.4)	25 (19-40)	2.0 (1.6-2.9)	*1480*	11	31 ± 15
66f	1.1 (0.9-1.3)	7.8 (4.7-16)	2.9 (2.1-4.0)	*1100*	3	4.8 ± 1.1

[a]IC$_{50}$ values based on single measurements are indicated in italics, other IC$_{50}$ values are the geometric mean of at least two measurements. Where sufficient data were available for calculation 95% confidence intervals are indicated in parenthesis. Data were obtained with a Fluorescence Imaging Plate Reader (FLIPR[®]) assay, see supporting information for detail.

[b]Single measurement

[c]In Wistar rats, po, 10 mg/kg, sacrifice after 1 h (mean ± SD, n = 3)

These six compounds were all potent triple blockers of the TTCCs (Table 11), and were selective against the Ca$_v$1.2 channel. Compounds **66a** and **66f** had low solubility in buffer and consequently lower systemic and brain exposures in rats after oral administration. Yet, the rather poorly soluble compound **66b** showed a good brain exposure. While the solubility in fasted state simulating intestinal fluids and in fed state simulating intestinal fluids remained moderate for compound **66a** (52 and 27 mg/L, respectively) and for compound **66f** (9 and 52 mg/L, respectively), these values were somewhat higher for compound **66b** (103 and 104 mg/L, respectively). Comparing compounds **66a** and **66b**, it should be noted that the introduction of the trifluoromethylcyclopropyl substituent[32] at position 4 of the phenethyl moiety was not triggered by an attempt to increase metabolic stability, which was good for both compounds (CL$_{int}$ in HLM = 6 and 24 μL/min/mg, respectively), but by standard SAR studies. On the other hand, compounds containing fluorine atoms, like compound **66b**, showed a slightly improved solubility profile, which was reflected in a better oral exposure. The beneficial effect of the ether substituent on solubility should be noticed as well, especially with compounds **66c**, **66d**, and **66e**. A longer chain at position 3 (compound **66f** vs. **66c**) led to a reduced solubility.

Compounds **66b**, **66c**, **66d**, and **66e** behaved similarly in metabolic stability, pharmacokinetics, and on their potential to inhibit CYP3A4 time-dependently (Table 12). They all displayed low intrinsic clearance in human liver microsomes. The IC$_{50}$-values measured after 30 min

preincubation remained relatively high and therefore unlikely to lead to drug-drug interactions. The in vivo clearances of compounds **66b**, **66c**, and **66e** were all similar, with excellent C_{max} and bioavailabilities. In an MDR1-MDCK assay, all compounds were well-permeable, but compound **66c** was a moderate pgp substrate, and was discarded at this stage.

Table 12. DMPK profile of four compounds.

Compound	CL_{int} HLM	MDR1[a]	3A4 shift and IC_{50}[b]	CL[c]	$T_{1/2}$[c]	C_{max}[d]	F[e]
	in μL/min/mg	in 10^6 cm/s	in μM	in mL/min/kg	in h	in nM	in %
66b	24	18/54/3.0	>2.2/46	24	2.5	1900	75
66c	28	15/68/4.5	>3.3/46	11	2.1	7300	132
66d	42	19/60/3.2	>4.4/23	-	-	-	-
66e	58	30/59/2.0	>5.9/17	11	3.7	6500	95

[a] At a concentration of 1 μM; $P_{appA\rightarrow B}$/ $P_{appB\rightarrow A}$/Ratio; ratio without units

[b] With testosterone as substrate; shift in IC_{50} after 30 min preincubation

[c] In Wistar rats at a dose of 1 mg/kg iv

[d] In plasma of Wistar rats at a dose of 10 mg/kg po

[e] Bioavailability

Compounds **66b**, **66d**, and **66e** were progressed for in vivo pharmacological characterization. They were screened in two rodent models: The WAG/Rij rat model of absence-like epilepsy, and the audiogenic seizure-sensitive (AGS) juvenile DBA/2J mouse model of generalized convulsive seizures[33]. In WAG/Rij rats, 10 mg/kg *po* of **66b**, **66d**, or **66e** significantly decreased the cumulative duration of absence-like seizures over the next 12 h period by 93, 35 and 79%

respectively compared to a matched vehicle group (p < 0.001 for **66b** and **66e** and p < 0.01 for **66d**, paired t-test, Figure 5a, 5c, 5e). Compounds **66b** and **66e** completely suppressed the absence-type seizures over the first 6 h following administration (Figure 5a, 5e). In the AGS model, juvenile DBA/2J mice were exposed to an auditory stimulus of maximum 60 sec or until the mouse showed tonic extension of the hind limbs. The test was performed 1 h or 3 h following oral administration of the compound and the severity of the seizure assessed *via* a behavioral scale, where seizure stage 0 is a normal behavior; stage 1, a wild running; stage 2, a clonic seizure and stage 3, the tonic extension of the hind limbs. In this model, compounds **66b** and **66e** showed a significant decrease of the seizure severity at a dose of 100 mg/kg *po* (p < 0.001 for both compounds, Mann-Whitney test), compound **66d** showed no efficacy, even at a dose of 300 mg/kg (Figure 5b, 5d, 5f). Blood and brain samples collected at the end of the test showed twice lower free brain exposure for compound **66d** than for compounds **66b** and **66e**. This result, combined with lower efficacy in the WAG/Rij rat model, led us to abandon this compound. Both **66b** and **66e** showed excellent efficacy in the WAG/Rij rat model (Figure 5) making their differentiation difficult. However, upon further profiling, compound **66b** showed lower covalent binding to protein (72 pmol/mg·h) than compound **66e** (207 pmol/mg·h) upon metabolic activation by human liver microsomes, triggering the selection of compound **66b** for further characterization.
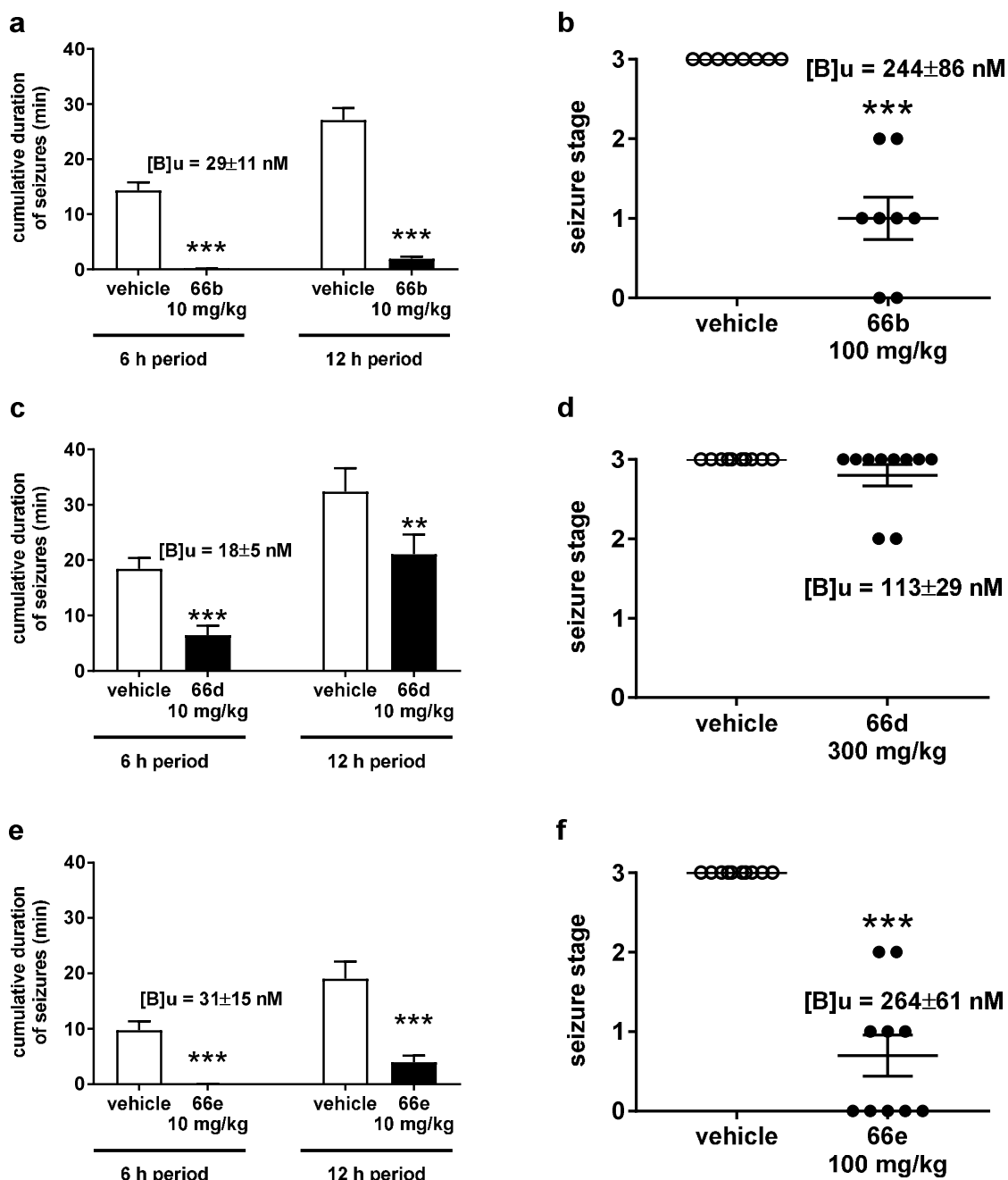
Figure 5: Impacts of compounds **66b**, **66d** and **66e** on the cumulative duration of absence

seizures in the male WAG/Rij rats model (a, c, e, respectively; n = 6 to 8 per group) and on

seizure severity in the audiogenic seizure-sensitive juvenile DBA/2J mouse model (b, d, f

respectively, n = 8 to 10 per group). Data are expressed as mean ± SEM. In the mouse model, seizure stage 0 = normal behavior, 1 = wild running, 2 = clonic seizure and 3 = tonic exension of the hind limbs. Mice were sacrificed just after their response to the auditory stimulus and brain sampled to allow the measurement of brain concentration. *, $p < 0.05$; **, $p < 0.01$; ***, $p < 0.001$ compared to vehicle (10% PEG400 + 90 % MC 0.5%) treated animals (paired t-test for a, c and e and Mann-Whitney test for b, d and f). $[B]_u$ = free brain concentration 1 h post administration in Wistar rats (mean ± SD, n = 3) (a, c, e) and 1 h (d, f) or 3 h (b) post administration in the mouse model (mean ± SD, n = 8 to 10). Baseline values (in min) for (a) 6 h period, **66b**, 18 ± 2 vs. veh., 17 ± 1; 12 h period, **66b**, 30 ± 2 vs. veh., 29 ± 2; (c) 6 h period, **66d**, 19 ± 3 vs. veh., 18 ± 2; 12 h period, **66d**, 32 ± 4 vs. veh., 30 ± 3; (e) 6 h period, **66e**, 16 ± 2 vs. veh., 14 ± 1; 12 h period, **66e**, 24 ± 2 vs. veh., 24 ± 3.

Final characterization of compound 66b. Compound **66b** was shown to be negative in an *Ames* test. Compound **66b** was profiled on rat and mice, dog, and cynomolgus TTCCs (Table 13) and no large species differences were observed.

Table 13. IC$_{50}$-values[a] of compound **66b** in different species.

Channel	Rat in nM	Mouse in nM	Dog in nM	Cynomolgus in nM
Ca$_v$3.1	16 (13-20)	6.4 (5-10)	20 (17-25)	n.d
Ca$_v$3.2	13 (10-16)	40 (31-56)	33 (26-48)	19 (14-31)
Ca$_v$3.3	1.8 (1.4-2.4)	n.d	3.4 (2.9-4.2)	n.d

[a] IC$_{50}$ values are the geometric mean of five to fifteen measurements. 95% confidence intervals are indicated in parenthesis. n.d: no data. Data were obtained with a Fluorescence Imaging Plate Reader (FLIPR®) assay, see supporting information for chetail.

The selectivity of compound **66b** was assessed against a panel of human cardiac and neuronal ion channels using patch-clamp and recombinant channels (hCa$_v$3.3, hCa$_v$1.2, hCa$_v$1.3, and hCa$_v$2.1; hK$_v$1.5, hK$_v$4.3/hKChIP2, hK$_v$7.1/minK, hK$_v$7.2/7.3, hK$_v$11.1-hERG, hHCN4, hKir2.1, hKir3.1/3.4; hNa$_v$1.1, hNa$_v$1.2, hNa$_v$1.5, and hNa$_v$1.6). Compound **66b** blocked hCa$_v$3.3 potently but with marked voltage-dependency (Kr ∼ 1500 nM and Ki ∼ 20 nM, consistent with the measurements using fluorescent dyes). Compound **66b** blocked the three other calcium channels (Ca$_v$1.2, Ca$_v$1.3, and Ca$_v$2.1) much less potently (<20% block at 10 μM from negative holding voltages). The inhibitory effect of compound **66b** on currents through other channels except hK$_v$11.1, hK$_v$1.5, and hK$_v$4.3/hKChIP2 was also <20 % at 10 μM; it was ∼30% for hKv1.5 and hK$_v$4.3/hKChIP2. Finally, compound **66b** blocked currents through hK$_v$11.1-hERG channels with an IC$_{50}$ of 5.5 μM.

The selectivity of compound **66b** was also assessed against sodium and potassium channels in rat cortical neurons using patch-clamp. Compound **66b** blocked currents through these channels weakly at 10 μM (<5% for sodium and <15% for potassium). Two hundred seventy-three other potential off-target proteins were screened at a concentration of 10 μM compound **66b** and a variety of techniques, including radioligand- binding assays and functional FLIPR assays. These proteins included G-protein-coupled receptors, enzymes, transporters, and nuclear receptors. An inhibition greater than 50% was observed for the following targets: calcium sensing receptor (84%), hERG ion channel (60%), tachykinin 2 receptor (60%), urotensin 2 receptor (60%), neuromedin U receptor 1 (56%), sigma 1 receptor (54%), and LPA3 receptor (55%).

The cardiovascular effects of compound **66b** were evaluated using ECG/BP telemetry in rats (normotensive Wistar and spontaneously-hypertensive Wistar-Kyoto, SHR), Dunkin-Hartley guinea pigs, Beagle dogs, and Cynomolgus monkeys following single oral administration (Table

14). During the 24h following administration, compound **66b** induced a minimal to slight decrease of HR in rats and monkeys but a slight increase in dogs and no effect in guinea pigs. BP was decreased slightly in rats and monkeys but was unchanged in dogs or guinea pigs. On the ECG, the PR-interval was unchanged in non-rodent species but it increased up to 13% in rats and a very low incidence of one to five 2nd-degree AV blocks per 15000 heart beats (Wenckebach or Mobitz II) was identified (Figure 6). No changes in the corrected QT-interval or the QRS-interval was seen in any species. The observed species differences in cardiovascular effects may be related to the higher heart rates of rats and the fact that drug-induced PR-interval prolongation is in general HR dependent[34] and/or to species-specific expression of TTCCs[35].

Table 14. Effect of oral administration of compound **66b** on cardiovascular parameters in conscious freely moving animals. Values are maximal vehicle-corrected changes from pre-dose and only statistically-significant changes are shown (ns: not significant, nd: not determined; MAP for mean arterial pressure, HR for heart rate; PR, QRS, QTc are the corresponding intervals in the electrocardiogram).

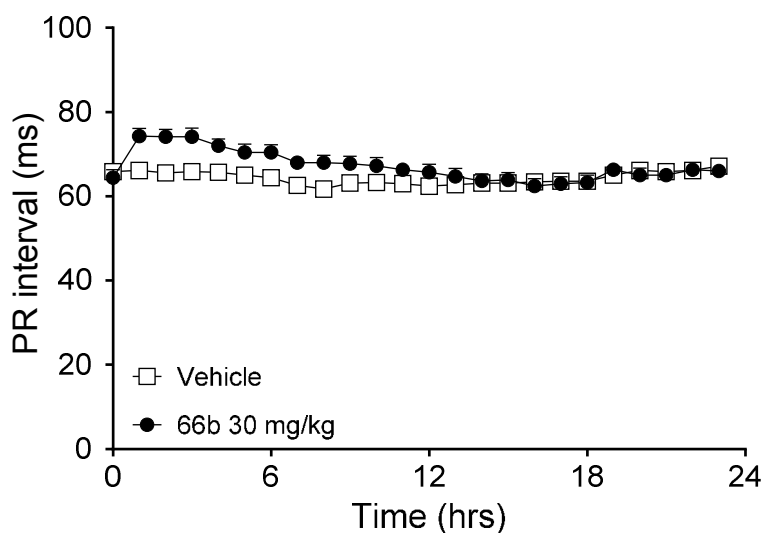| Species	MAP	HR	PR	QRS	QTc	Dose mg/kg	$C_{u,max}$ nM
Wistar rat	-7%	-10%	13%	ns	nd	30	190
SHR	-8%	-13%	13%	ns	nd	30	90
Guinea pig	ns	ns	ns	ns	ns	30	140
Dog	ns	15%	ns	ns	ns	10	140
Cynomolgus	-13%	17%	ns	ns	ns	1000	160
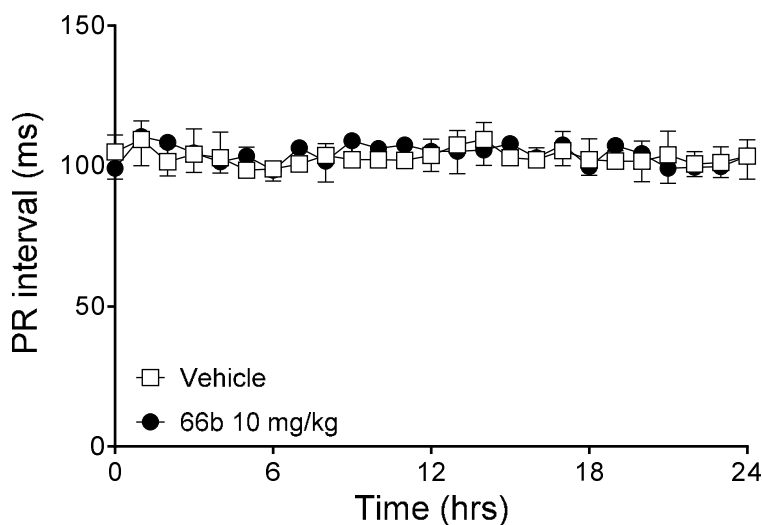
Figure 6: Effect of oral administration of compound **66b** (●) or vehicle (□, 10% PEG400 + 90 % MC 0.5%) on PR-intervals in conscious freely moving male Beagle dogs (A) or male SHR rats (B). Compound (10 mg/kg for dogs and 30 mg/kg for rats) or vehicle was administered at time 0 and data are represented as mean ± SEM (n = 4 per group for dogs and n = 7-8 per group for rats).

Table 15. IC$_{50}$-values of compound **66b** on main P450 enzymes (all values in μM).

1A2	2A6	2B6	2C8	2C9	2C19	2D6	3A4
>100	>100	52	14	22	25	15	51

The potential of compound **66b** to cause drug-drug interactions was assessed by studying the inhibition of the main P450 enzymes (Table 15). No time-dependent P450 inhibition was observed. Because the IC$_{50}$-values for inhibiting P450 enzymes are much higher than needed for the pharmacological effect, the P450 inhibition potential of **66b** is predicted to be low.

In order to predict the human PK of compound **66b**, the clearance was predicted from microsomes (and rat hepatocytes) and compared to the clearance in mouse, dog and monkey after iv dosing at 1 mg/kg body weight (Table 16).

Table 16. Unbound fractions and clearance for **66b** in different species.

Species	$f_{u,plasma}$	CL$_{int}$ (liver microsomes) μL/min/mg protein	Predicted CL mL/min/kg	Observed CL mL/min/kg
Mouse	0.012	18	1.1	13
Rat	0.031	59	2.2	29
Dog	0.040	1.8	0.08	0.9
Monkey	0.047	9.0	0.54	5.5
Human	0.026	3.7	0.21	?

An about 10-fold underprediction of clearance was found for mouse, rat, dog and monkey. Therefore, the approach for human clearance prediction in man was estimated by allometric scaling from experimentally determined clearance in mouse, rat, dog and monkey with correction

of species differences in plasma protein binding. The relationship between clearance and body weight is given in Figure 7, together with the predicted human clearance (0.22 mL/min/kg body weight).
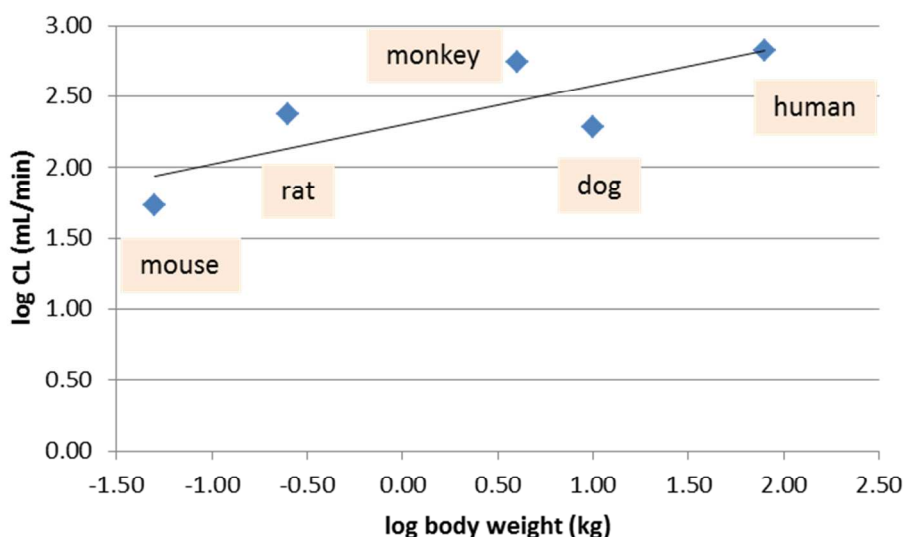

Figure 7. Allometric scaling of compound **66b**.

Both extrapolated CL_{int} from liver microsomes as well as allometric scaling from observed animal CL resulted in a low predicted clearance of compound **66b** in man, making this compound a suitable candidate antiepileptic drug.

CONCLUSIONS

In summary, we reported here the discovery and pharmacological characterization of pyrazole carboxamides as a new class of selective, potent, brain penetrant T-type calcium channel blockers. First SAR studies led to compound **6j** as a triple, potent TTCC blocker that showed excellent efficacy in the WAG/rij rat model for absence epilepsies. The search for a fine balance

between solubility, metabolic stability, and active efflux led to further optimization of the *para*-position at the phenylacetic acid moiety (compounds **16l** or **16p**). At this stage, it was observed that the amide bond of these compounds was slowly hydrolyzed in human plasma, releasing an *Ames*-positive aminopyrazole as metabolite. Different approaches to circumvent this issue (increased steric hindrance close to the amide bond, introduction of a non-aromatic amine moiety, reversing the amide bond functionality, replacement of the pyrazole moiety by other heteroaryls) failed. Eventually, the aminopyrazole **57k** was identified as an Ames-negative aminopyrazole that could be introduced successfully into compounds that would display excellent overall properties. After final optimization, we identified compound **66b** as being suitable for clinical development. This compound entered phase 1 clinical trials and further reports will describe this development in due time.

EXPERIMENTAL SECTION

All reagents and solvents were used as purchased from commercial sources (Sigma-Aldrich Switzerland, Lancaster Synthesis GmbH, Germany, Acros Organics USA, ABCR GmbH Germany, ArkPharm Inc USA). Metal catalysts were generally purchased from Strem chemicals. Unless specified otherwise, all reactions were conducted under an inert atmosphere (N_2 or Ar). Progress of the reactions was followed either by thin-layer chromatography (TLC) analysis (Merck, 0.2 mm silica gel 60 F254 on glass plates) and/or by LC-MS. Unless specified otherwise, all prepared compounds were > 95% pure (LC-MS). Unless stated otherwise, all compounds possess a purity of > 95%. Particular attention was paid to the 3-amino-1-benzylpyrazoles and other aminoheteroaryls sent to an Ames test; in such cases, only samples that display impurities neither on the LC-trace nor by ^{1}H-NMR were released for this test. [1]H-

NMR spectra were recorded at rt with a Brucker NMR 500 spectrometer [1]H (500 MHz) equipped with a Bruker's DCH cryoprobe. Alternatively, they were recorded at a 400MHz Ultra Shield NMR from Brucker with Avance 25mm PABBO BB-1H/D room temperature probe head. Spectra recorded at 300 MHz were recorded on a Varian Gemini 300. Chemical shifts are reported in ppm downfield from tetramethylsilane using residual solvent signals as internal reference. The multiplicity is described as singlet s, doublet d, triplet t, quadruplet q, quintuplet quint, hextet h, heptuplet hept, multiplet m. LC-MS Unless notified otherwise, the following conditions were used for analytical LC-MS data: Zorbax SB-Aq column, 3.5 μm, 4.6 x 50 mm, 5% CH_3CN / 95% H_2O with 0.04% TFA → 100% CH_3CN over 1.0 min, 4.5 mL/min. Automated FC: classical flash chromatography is often replaced by automated systems. This does not change the separation process *per se*. A person skilled in the art will be able to replace a classical FC process by an automated one, and *vice versa*. Typical automated systems can be used, as they are provided by Büchi, Isco (Combiflash), or Biotage for instance.

tert-Butyl 2-(4-(1-(trifluoromethyl)cyclopropyl)phenyl)acetate (**17u**). A mixture of 1-bromo-4-(1-(trifluoromethyl)cyclopropyl)benzene (8.00 g, 30.2 mmol), 2-*tert*-butoxy-2-oxoethylzinc chloride (0.5 M, in Et_2O, 84.6 mL, 30.2 mmol), $Pd_2(dba)_3$ (553 mg, 0.604 mmol), and X-PHOS (288 mg, 0.604 mmol) in THF (160 mL) was stirred overnight at 90 °C. The mixture is allowed to cool to rt, and the solvents are removed under reduced pressure. Purification of the crude by automated FC (EtOAc / heptane 6:94, 330 g silicagel) yielded the title product (8.72 g, 96%). ^{1}H-NMR ($CDCl_3$, 500 MHz): 7.43 (d, J = 8.1 Hz, 2H), 7.27 (d, J = 8.1 Hz, 2H), 3.55 (s, 2H), 1.47 (s, 9H), 1.35 (m, 2H), 1.04 (m, 2H). LC-MS: t_R = 1.01 min.

2-(4-(1-(Trifluoromethyl)cyclopropyl)phenyl)acetic acid (**18u**). A sol. of compound **17u** (4.30 g, 14.3 mmol) in HCOOH (27 mL) was stirred at rt overnight. The solvents were removed under reduced pressure, which yielded the crude title product (3.47 g). LC-MS: t_R = 0.81 min.

6-((3-Amino-1H-pyrazol-1-yl)methyl)nicotinonitrile (**57k**). K_2CO_3 (25.0 g, 181 mmol) was added to a mixture of 6-bromomethyl-nicotinonitrile (7.50 g, 36.2 mmol), 5-nitro-1*H*-pyrazole (4.09 g, 36.2 mmol) and Bu_4NBr (2.33 g, 7.23 mmol) in acetone (210 mL) at rt. The mixture was stirred at rt for 2.5 h. The reaction mixture was filtered, rinsed with acetone, and the solvents were removed under reduced pressure. Purification of the crude by automated FC (EtOAc / heptane 0:100 → 70:30, 120g silicagel) yielded 6-((3-nitro-1*H*-pyrazol-1-yl)methyl)nicotinonitrile (5.23 g, 63%). R_f = 0.20 (EtOAc / heptane 1:1). ^{1}H-NMR (CDCl$_3$, 500 MHz): 8.87 (d, J = 1.4 Hz, 1H), 8.02 (dd, J_1 = 8.1 Hz, J_2 = 2.1 Hz, 1H), 7.70 (d, J = 2.5 Hz, 1H), 7.39 (d, J = 8.1 Hz, 1H), 7.00 (d, J = 2.5 Hz, 1H), 5.58 (s, 2H). LC-MS: t_R = 0.66 min, MH$^+$ = 230.15.

To a EtOH / H_2O mixture (2:1, 180 mL) were added in sequence the former product (5.23 g, 2.28 mmol), Fe (powder 325 mesh, 6.3 g, 114 mmol), and NH_4Cl (6.10 g, 114 mmol). The dark suspension was heated to 75°C for 1.5 h. The mixture was allowed to cool to rt. The mixture was filtered through Celite$^®$, and rinsed with EtOH. The light yellow filtrate was evaporated under reduced pressure. The residue was partitioned between CH_2Cl_2 and water. The aq. layer was extracted with CH_2Cl_2 (3x). The combined org. extracts were dried over Na_2SO_4, filtered, and the solvents were removed under reduced pressure to yield the title product (4.32 g, 95%). ^{1}H-NMR (CDCl$_3$, 500 MHz): 8.85 (d, J = 1.4 Hz, 1H), 7.92 (dd, J_1 = 8.1 Hz, J_2 = 2.1 Hz, 1H), 7.32 (d, J = 2.3 Hz, 1H), 7.09 (d, J = 8.1 Hz, 1H), 5.73 (d, J = 2.3 Hz, 1H), 5.31 (s, 2H), 3.71 (broad, s, 2H). LC-MS: t_R = 0.40 min, MH$^+$ = 200.21.

N-(1-((5-Cyanopyridin-2-yl)methyl)-1H-pyrazol-3-yl)-2-(4-(1-(trifluoromethyl)cyclopropyl)-phenyl)acetamide (**66b**). At rt, compound **18u** (10.0 g, 41.1 mmol) was dissolved in CH_3CN (280 mL). DIPEA (15.5 mL, 90.4 mmol) and HATU (16.4 g, 43.1 mmol) were added. The yellow sol. was stirred for 5 min, and compound **57k** (8.55 g, 41.1 mmol) was added. The mixture was stirred at rt overnight. The solvents were removed under reduced pressure, and the residue was taken up in EtOAc, and washed with aq. 0.1M HCl (1x), with aq. sat. $NaHCO_3$ (1x) and with H_2O (1x). The org. layer was dried over Na_2SO_4, filtered, and the solvents were removed under reduced pressure. Purification of the crude by automated FC (EtOAc / heptane 0:100 → 100:0, 330 g silicagel) yielded a solid that was recrystallized from toluene to yield the title product (10.7 g, 58%). ^{1}H-NMR (d_6-DMSO, 500 MHz): 10.75 (s, 1H), 8.99 (s, 1H), 8.29 (d, J = 7.9 Hz, 1H), 7.80 (s, 1H), 7.40 (d, J = 8.3 Hz, 2H), 7.32 (d, J = 8.3 Hz, 2H), 7.19 (d, J = 8.1 Hz, 1H), 6.54 (s, 1H), 5.45 (s, 2H), 3.60 (s, 2H), 1.31 (s, 2H), 1.09 (s, 2H). LC-MS: t_R = 0.87, MH^+ = 426.14.

AUTHOR INFORMATION

Corresponding Author

*Olivier Bezençon, Idorsia Pharmaceuticals Ltd, Hegenheimermattweg 91, CH – 4123 Allschwil. Tel. +41 61 565 65 77. Email: olivier.bezencon@idorsia.com

Present Addresses

†Thomas Pfeifer: ADME & more, Marktweg 30, D-79576 Weil¨am Rhein, Germany

ACKNOWLEDGMENT

ABBREVIATIONS

Ac, acetyl; aq., aqueous; Bn, benzyl; BP, blood pressure; Bu, butyl, C, concentration; Cl, clearance; COD, cyclooctadiene; CSF, cerebrospinal fluid; CL, clearance; CL_{int}, intrinsic clearance, DAST, (diethylamino)sulfur trifluoride; dba, dibenzylideneacetone; DBU, diazabicyclo[5.4.0]undec-7-ene; DEAD, diethyl azodicarboxylate; DIBAL-H, diisobutylaluminium hydride; DIPEA, diisopropylethylamine; DMA, *N,N*-dimethylacetamide, DMAP, 4-(*N,N*-dimethylamino)pyridine; DMF, *N,N*-dimethylformamide, DMSO, dimethylsulfoxide; DMPK, drug metabolism and pharmacokinetics; DPPA, diphenyl phosphoryl azide; DPPP, 1,3-bis(diphenylphosphino)propane ECG, electrocardiogram; EEG, electroencephalogram; EDC·HCl, 1-ethyl-3-(3-dimethylaminopropyl)carbodiimide hydrochloride salt; eq., equivalent; Et, ethyl; F, bioavailability; FaSSIF, fasted state simulated intestinal fluid; FC, flash chromatography; FeSSIF, fed state simulated intestinal fluid;; FLIPR, fluorescence imaging plate reader; GPCR, G-protein coupled receptor; HATU, 1-[bis(dimethylamino)methylene]-1H-1,2,3-triazolo[4,5-b]pyridinium 3-oxid hexafluorophosphate

(CAS No 148893-10-1); HBTU, *O*-benzotriazole-N,N,N',N'-tetramethyl-uronium-hexafluoro-phosphate (CAS No 94790-37-1); HLM, human liver microsomes; HPLC, high performance liquid chromatography; HR, heart rate; LC, liquid chromatography; MC, methylcellulose ; mdr1, multidrug resistance protein 1; Me, methyl; MH^+, mass of the protonated molecule; MS, mass spectroscopy; Ms, mesyl (CH_3SO_2-); NMR, nuclear magnetic resonance; org., organic; PEG, polyethylene glycol; PEPPSI-IPr, 1,3-bis(2,6-diisopropylphenyl)imidazolidene)-(3-chloropyridyl)palladium(II)dichloride; pgp, p-glycoprotein; Ph, phenyl; quant., quantitative; QPhos, 1,2,3,4,5-pentaphenyl-1'-(di-tert-butylphosphino)ferrocene (CAS No 312959-24-3); rac., racemic; R_f, retention index; RLM, rat liver microsome; rt, room temperature; SAR, structure activity relationship; ^{t}Bu, tert-butyl; TBTU, *N,N,N',N'*-tetramethyl-*O*-(benzotriazol-1-yl)uranium tetrafluoroborate; TEA, triethylamine; TFA, trifluoroacetic acid; Tf_2O, trifluoromethanesulfonic anhydride; THF, tetrahydrofuran; TLC, thin layer chromatography; TMS, trimethylsilyl; t_R, retention time; Ts, tosyl; TTCC, T-type calcium channel; veh.: vehicle; vs.: versus; X-PHOS, 2-dicyclohexylphosphino-2',4',6'-triisopropylbiphenyl (CAS No 564483-18-7).

ASSOCIATED CONTENT

Supporting Information. All experimental details and molecular formula strings can be found in the supporting information. This material is available free of charge *via* the Internet at http://pubs.acs.org.

REFERENCES

1.   Zamponi, G. W.; Striessnig, J.; Koschak, A.; Dolphin, A. C. The physiology, pathology, and pharmacology of voltage-gated calcium channels and their future therapeutic potential. *Pharmacol. Rev.* **2015,** *67*, 821-870.

2.   Clozel, J. P.; Ertel, E. A.; Ertel, S. I. Discovery and main pharmacological properties of mibefradil (Ro 40-5967), the first selective T-type calcium channel blocker. *J. Hypertens. Suppl.* **1997,** *15*, S17-25.

3.   (a) Xie, X.; Van Deusen, A. L.; Vitko, I.; Babu, D. A.; Davies, L. A.; Huynh, N.; Cheng, H.; Yang, N.; Barrett, P. Q.; Perez-Reyes, E. Validation of high throughput screening assays against three subtypes of Ca_v3 T-type channels using molecular and pharmacologic approaches. *Assay Drug Dev. Technol.* **2007,** *5*, 191-203; (b) Belardetti, F.; Tringham, E.; Eduljee, C.; Jiang, X.; Dong, H.; Hendricson, A.; Shimizu, Y.; Janke, D. L.; Parker, D.; Mezeyova, J.; Khawaja, A.; Pajouhesh, H.; Fraser, R. A.; Arneric, S. P.; Snutch, T. P. A fluorescence-based high-throughput screening assay for the identification of T-type calcium channel blockers. *Assay Drug Dev. Technol.* **2009,** *7*, 266-280.

4.   (a) Viana, F.; Van den Bosch, L.; Missiaen, L.; Vandenberghe, W.; Droogmans, G.; Nilius, B.; Robberecht, W. Mibefradil (Ro 40-5967) blocks multiple types of voltage-gated calcium channels in cultured rat spinal motoneurones. *Cell Calcium* **1997,** *22*, 299-311; (b) Benjamin, E. R.; Pruthi, F.; Olanrewaju, S.; Shan, S.; Hanway, D.; Liu, X.; Cerne, R.; Lavery, D.; Valenzano, K. J.; Woodward, R. M.; Ilyin, V. I. Pharmacological characterization of recombinant N-type calcium channel ($Ca_v2.2$) mediated calcium mobilization using FLIPR. *Biochem. Pharmacol.* **2006,** *72*, 770-782.

5.   McNulty, M. M.; Hanck, D. A. State-dependent mibefradil block of Na$^+$ channels. *Mol. Pharmacol.* **2004,** *66*, 1652-1661.

6.   (a) Egan, M. F.; Zhao, X.; Smith, A.; Troyer, M. D.; Uebele, V. N.; Pidkorytov, V.; Cox, K.; Murphy, M.; Snavely, D.; Lines, C.; Michelson, D. Randomized controlled study of the T-type calcium channel antagonist MK-8998 for the treatment of acute psychosis in patients with schizophrenia. *Hum. Psychopharmacol.* **2013,** *28*, 124-133; (b) Zamponi, G. W. Targeting voltage-gated calcium channels in neurological and psychiatric diseases. *Nat. Rev. Drug Discovery* **2016,** *15*, 19-34.

7.   (a)   ClinicalTrials.gov   web   site, https://clinicaltrials.gov/ct2/show/NCT03101241?term=CX-8998&rank=1 (accessed October 19, 2017); (b) Company Web Page, Cavion, http://cavionpharma.com/technology-and-platform (accessed December 23, 2015).

8.   (a) Siegrist, R.; Pozzi, D.; Jacob, G.; Torrisi, C.; Colas, K.; Braibant, B.; Mawet, J.; Pfeifer, T.; de Kanter, R.; Roch, C.; Kessler, M.; Corminboeuf, O.; Bezençon, O. Structure-activity relationship, drug metabolism and pharmacokinetics properties optimization, and in vivo studies of new brain penetrant triple T-type calcium channel blockers. *J. Med. Chem.* **2016,** *59*, 10661-10675; (b) Remeň, L.; Bezençon, O.; Simons, L.; Gaston, R.; Downing, D.; Gatfield, J.; Roch, C.; Kessler, M.; Mosbacher, J.; Pfeifer, T.; Grisostomi, C.; Rey, M.; Ertel, E. A.; Moon, R. Preparation, antiepileptic activity, and cardiovascular safety of dihydropyrazoles as brain-penetrant T-type calcium channel blockers. *J. Med. Chem.* **2016,** *59*, 8398-8411; (c) Shipe, W. D.; Barrow, J. C.; Yang, Z. Q.; Lindsley, C. W.; Yang, F. V.; Schlegel, K. A.; Shu, Y.; Rittle, K. E.; Bock, M. G.; Hartman, G. D.; Tang, C.; Ballard, J. E.; Kuo, Y.; Adarayan, E. D.;

Prueksaritanont, T.; Zrada, M. M.; Uebele, V. N.; Nuss, C. E.; Connolly, T. M.; Doran, S. M.; Fox, S. V.; Kraus, R. L.; Marino, M. J.; Graufelds, V. K.; Vargas, H. M.; Bunting, P. B.; Hasbun-Manning, M.; Evans, R. M.; Koblan, K. S.; Renger, J. J. Design, synthesis, and evaluation of a novel 4-aminomethyl-4-fluoropiperidine as a T-type Ca^{2+} channel antagonist. *J. Med. Chem.* **2008,** *51*, 3692-3695; (d) Tringham, E.; Powell, K. L.; Cain, S. M.; Kuplast, K.; Mezeyova, J.; Weerapura, M.; Eduljee, C.; Jiang, X.; Smith, P.; Morrison, J. L.; Jones, N. C.; Braine, E.; Rind, G.; Fee-Maki, M.; Parker, D.; Pajouhesh, H.; Parmar, M.; O'Brien, T. J.; Snutch, T. P. T-type calcium channel blockers that attenuate thalamic burst firing and suppress absence seizures. *Sci. Transl. Med.* **2012,** *4*, 1-13; (e) Casillas-Espinosa, P. M.; Hicks, A.; Jeffreys, A.; Snutch, T. P.; O'Brien, T. J.; Powell, K. L. Z944, a novel nelective T-type calcium channel antagonist delays the progression of seizures in the amygdala kindling model. *PLoS One* **2015,** *10*, e0130012; (f) Yang, Z. Q.; Barrow, J. C.; Shipe, W. D.; Schlegel, K. A.; Shu, Y.; Yang, F. V.; Lindsley, C. W.; Rittle, K. E.; Bock, M. G.; Hartman, G. D.; Uebele, V. N.; Nuss, C. E.; Fox, S. V.; Kraus, R. L.; Doran, S. M.; Connolly, T. M.; Tang, C.; Ballard, J. E.; Kuo, Y.; Adarayan, E. D.; Prueksaritanont, T.; Zrada, M. M.; Marino, M. J.; Graufelds, V. K.; DiLella, A. G.; Reynolds, I. J.; Vargas, H. M.; Bunting, P. B.; Woltmann, R. F.; Magee, M. M.; Koblan, K. S.; Renger, J. J. Discovery of 1,4-substituted piperidines as potent and selective inhibitors of T-type calcium channels. *J. Med. Chem.* **2008,** *51*, 6471-6477.

9.   Yang, Z.-Q.; Schlegel, K.-A. S.; Shu, Y.; Reger, T. S.; Cube, R.; Mattern, C.; Coleman, P. J.; Small, J.; Hartman, G. D.; Ballard, J.; Tang, C.; Kuo, Y.; Prueksaritanont, T.; Nuss, C. E.; Doran, S.; Fox, S. V.; Garson, S. L.; Li, Y.; Kraus, R. L.; Uebele, V. N.; Taylor, A. B.; Zeng, W.; Fang, F.; Chavez-Eng, C.; Troyer, M. D.; Luk, J. A.; Laethem, T.; Cook, W. O.; Renger, J.

J.; Barrow, J. C. Short-acting T-type calcium channel antagonists significantly modify sleep architecture in rodents. *ACS Med. Chem. Lett.* **2010,** *1*, 504-509.

10. Uslaner, J. M.; Smith, S. M.; Huszar, S. L.; Pachmerhiwala, R.; Hinchliffe, R. M.; Vardigan, J. D.; Nguyen, S. J.; Surles, N. O.; Yao, L.; Barrow, J. C.; Uebele, V. N.; Renger, J. J.; Clark, J.; Hutson, P. H. T-type calcium channel antagonism produces antipsychotic-like effects and reduces stimulant-induced glutamate release in the nucleus accumbens of rats. *Neuropharmacology* **2012,** *62*, 1413-1421.

11. (a) Yang, Y. C.; Tai, C. H.; Pan, M. K.; Kuo, C. C. The T-type calcium channel as a new therapeutic target for Parkinson's disease. *Pfluegers Arch.* **2014,** *466*, 747-755; (b) Xiang, Z.; Thompson, A. D.; Brogan, J. T.; Schulte, M. L.; Melancon, B. J.; Mi, D.; Lewis, L. M.; Zou, B.; Yang, L.; Morrison, R.; Santomango, T.; Byers, F.; Brewer, K.; Aldrich, J. S.; Yu, H.; Dawson, E. S.; Li, M.; McManus, O.; Jones, C. K.; Daniels, J. S.; Hopkins, C. R.; Xie, X. S.; Conn, P. J.; Weaver, C. D.; Lindsley, C. W. The discovery and characterization of ML218: a novel, centrally active T-type calcium channel inhibitor with robust effects in STN neurons and in a rodent model of Parkinson's disease. *ACS Chem. Neurosci.* **2011,** *2*, 730-742; (c) Miwa, H.; Koh, J.; Kajimoto, Y.; Kondo, T. Effects of T-type calcium channel blockers on a parkinsonian tremor model in rats. *Pharmacol. Biochem. Behav.* **2011,** *97*, 656-659.

12. (a) Miwa, H.; Kondo, T. T-type calcium channel as a new therapeutic target for tremor. *Cerebellum* **2011,** *10*, 563-569; (b) Handforth, A.; Homanics, G. E.; Covey, D. F.; Krishnan, K.; Lee, J. Y.; Sakimura, K.; Martin, F. C.; Quesada, A. T-type calcium channel antagonists suppress tremor in two mouse models of essential tremor. *Neuropharmacology* **2010,** *59*, 380-387.

13.   Uebele, V. N.; Gotter, A. L.; Nuss, C. E.; Kraus, R. L.; Doran, S. M.; Garson, S. L.; Reiss, D. R.; Li, Y.; Barrow, J. C.; Reger, T. S.; Yang, Z. Q.; Ballard, J. E.; Tang, C.; Metzger, J. M.; Wang, S. P.; Koblan, K. S.; Renger, J. J. Antagonism of T-type calcium channels inhibits high-fat diet-induced weight gain in mice. *J. Clin. Invest.* **2009,** *119*, 1659-1667.

14.   Lee, M. Z944: a first in class T-type calcium channel modulator for the treatment of pain. *J. Peripher. Nerv. Syst.* **2014,** *19 Suppl 2*, S11-S12.

15.   (a) Lambert, R. C.; Bessaih, T.; Crunelli, V.; Leresche, N. The many faces of T-type calcium channels. *Pfluegers Arch.* **2014,** *466*, 415-423; (b) Crunelli, V.; David, F.; Leresche, N.; Lambert, R. C. Role for T-type Ca^{2+} channels in sleep waves. *Pfluegers Arch.* **2014,** *466*, 735-745; (c) Cheong, E.; Shin, H. S. T-type Ca^{2+} channels in normal and abnormal brain functions. *Physiol. Rev.* **2013,** *93*, 961-992; (d) Talley, E. M.; Cribbs, L. L.; Lee, J. H.; Daud, A.; Perez-Reyes, E.; Bayliss, D. A. Differential distribution of three members of a gene family encoding low voltage-activated (T-type) calcium channels. *J. Neurosci.* **1999,** *19*, 1895-1911.

16.   (a) Eckle, V. S.; Shcheglovitov, A.; Vitko, I.; Dey, D.; Yap, C. C.; Winckler, B.; Perez-Reyes, E. Mechanisms by which a CACNA1H mutation in epilepsy patients increases seizure susceptibility. *J. Physiol.* **2014,** *592*, 795-809; (b) Zamponi, G. W.; Lory, P.; Perez-Reyes, E. Role of voltage-gated calcium channels in epilepsy. *Pfluegers Arch.* **2010,** *460*, 395-403; (c) Powell, K. L.; Cain, S. M.; Ng, C.; Sirdesai, S.; David, L. S.; Kyi, M.; Garcia, E.; Tyson, J. R.; Reid, C. A.; Bahlo, M.; Foote, S. J.; Snutch, T. P.; O'Brien, T. J. A $Ca_v3.2$ T-type calcium channel point mutation has splice-variant-specific effects on function and segregates with seizure expression in a polygenic rat model of absence epilepsy. *J. Neurosci.* **2009,** *29*, 371-380; (d) Broicher, T.; Kanyshkova, T.; Meuth, P.; Pape, H. C.; Budde, T. Correlation of T-channel coding

gene expression, IT, and the low threshold Ca^{2+} spike in the thalamus of a rat model of absence epilepsy. *Mol. Cell. Neurosci.* **2008,** *39*, 384-399; (e) Heron, S. E.; Khosravani, H.; Varela, D.; Bladen, C.; Williams, T. C.; Newman, M. R.; Scheffer, I. E.; Berkovic, S. F.; Mulley, J. C.; Zamponi, G. W. Extended spectrum of idiopathic generalized epilepsies associated with CACNA1H functional variants. *Ann. Neurol.* **2007,** *62*, 560-568; (f) Khosravani, H.; Zamponi, G. W. Voltage-gated calcium channels and idiopathic generalized epilepsies. *Physiol. Rev.* **2006,** *86*, 941-966; (g) Talley, E. M.; Solorzano, G.; Depaulis, A.; Perez-Reyes, E.; Bayliss, D. A. Low-voltage-activated calcium channel subunit expression in a genetic model of absence epilepsy in the rat. *Brain Res. Mol. Brain Res.* **2000,** *75*, 159-165.

17. (a) Ernst, W. L.; Noebels, J. L. Expanded alternative splice isoform profiling of the mouse $Ca_v3.1/\alpha_{1G}$ T-type calcium channel. *BMC Mol. Biol.* **2009,** *10*, 53; (b) Song, I.; Kim, D.; Choi, S.; Sun, M.; Kim, Y.; Shin, H. S. Role of the alpha1G T-type calcium channel in spontaneous absence seizures in mutant mice. *J. Neurosci.* **2004,** *24*, 5249-5257; (c) Kim, D.; Song, I.; Keum, S.; Lee, T.; Jeong, M. J.; Kim, S. S.; McEnery, M. W.; Shin, H. S. Lack of the burst firing of thalamocortical relay neurons and resistance to absence seizures in mice lacking α_{1G} T-type Ca^{2+} channels. *Neuron* **2001,** *31*, 35-45.

18. Bezençon, O.; Remeň, L.; Richard, S.; Roch, C.; Kessler, M.; Moon, R.; Ertel, E. A.; Pfeifer, T.; Capeleto, B., Discovery and evaluation of $Ca_v3.1$-selective T-type calcium channel blockers. *Bioorg. Med. Chem. Lett.* [Online early access]. *DOI* 10.1016/j.bmcl.2017.09.063. Published online: October 3, 2017. http://www.sciencedirect.com/science/article/pii/S0960894X1730971X (accessed November 2, 2017).

19. Coenen, A. M.; Van Luijtelaar, E. L. Genetic animal models for absence epilepsy: a review of the WAG/Rij strain of rats. *Behav. Genet.* **2003,** *33*, 635-655.

20. (a) Ritchie, T. J.; Macdonald, S. J. The impact of aromatic ring count on compound developability--are too many aromatic rings a liability in drug design? *Drug Discovery Today* **2009,** *14*, 1011-1020; (b) Ritchie, T. J.; Macdonald, S. J.; Young, R. J.; Pickett, S. D. The impact of aromatic ring count on compound developability: further insights by examining carbo- and hetero-aromatic and -aliphatic ring types. *Drug Discovery Today* **2011,** *16*, 164-171; (c) Ritchie, T. J.; Macdonald, S. J. Physicochemical descriptors of aromatic character and their use in drug discovery. *J. Med. Chem.* **2014**, *57*, 7206-7215.

21. Barraclough, P.; Black, J. W.; Cambridge, D.; Firmin, D.; Gerskowitch, V. P.; Glen, R. C.; Giles, H.; Gillam, J. M.; Hull, R. A.; Iyer, R.; Randall, R.; Shah, G. P.; Smith,S.; Whiting, M. V. Inotropic polyazapentalene sulmazole analogues. *Arch. Pharm. (Weinheim)* **1992,** *325*, 225-234.

22. Robak, M. T.; Herbage, M. A.; Ellman, J. A. Synthesis and applications of *tert*-butanesulfinamide. *Chem. Rev.* **2010,** *110*, 3600-3740.

23. Aust, A. E.; Wold, S. A. Induction of bacterial mutations by aminopyrazoles, compounds which cause mammary cancer in rats. *Carcinogenesis* **1986,** *7*, 2019-2023.

24. Di Fabio, R.; St-Denis, Y.; Sabbatini, F. M.; Andreotti, D.; Arban, R.; Bernasconi, G.; Braggio, S.; Blaney, F. E.; Capelli, A. M.; Castiglioni, E.; Di Modugno, E.; Donati, D.; Fazzolari, E.; Ratti, E.; Feriani, A.; Contini, S.; Gentile, G.; Ghirlanda, D.; Provera, S.; Marchioro, C.; Roberts, K. L.; Mingardi, A.; Mattioli, M.; Nalin, A.; Pavone, F.; Spada, S.; Trist,

D. G.; Worby, A. Synthesis and pharmacological characterization of novel druglike corticotropin-releasing factor 1 antagonists. *J. Med. Chem.* **2008,** *51*, 7370-7379.

25. (a) Kazius, J.; McGuire, R.; Bursi, R. Derivation and validation of toxicophores for mutagenicity prediction. *J. Med. Chem.* **2005,** *48*, 312-320; (b) Colvin, M. E.; Hatch, F. T.; Felton, J. S. Chemical and biological factors affecting mutagen potency. *Mutat. Res.* **1998,** *400*, 479-492.

26. Leach, A. G.; McCoull, W.; Bailey, A.; Barton, P.; Mee, C.; Rosevere, E. Experimental testing of quantum mechanical predictions of mutagenicity: aminopyrazoles. *Chem. Res. Toxicol.* **2013,** *26*, 703-709.

27. Benigni, R.; Passerini, L.; Gallo, G.; Giorgi, F.; Cotta-Ramusino, M. QSAR models for discriminating between mutagenic and nonmutagenic aromatic and heteroaromatic amines. *Environ. Mol. Mutagen.* **1998,** *32*, 75-83.

28. (a) McCarren, P.; Bebernitz, G. R.; Gedeck, P.; Glowienke, S.; Grondine, M. S.; Kirman, L. C.; Klickstein, J.; Schuster, H. F.; Whitehead, L. Avoidance of the Ames test liability for aryl-amines via computation. *Bioorg. Med. Chem* .**2011,** *19*, 3173-3182; (b) McCarren, P.; Springer, C.; Whitehead, L. An investigation into pharmaceutically relevant mutagenicity data and the influence on Ames predictive potential. *J. Cheminf.* **2011,** *3*, 51; (c) Bentzien, J.; Hickey, E. R.; Kemper, R. A.; Brewer, M. L.; Dyekjaer, J. D.; East, S. P.; Whittaker, M. An in silico method for predicting Ames activities of primary aromatic amines by calculating the stabilities of nitrenium ions. *J. Chem. Inf. Model.* **2010,** *50*, 274-297.

29. (a) Debnath, A. K.; Debnath, G.; Shusterman, A. J.; Hansch, C. A QSAR investigation of the role of hydrophobicity in regulating mutagenicity in the Ames test: 1. Mutagenicity of

aromatic and heteroaromatic amines in Salmonella typhimurium TA98 and TA100. *Environ. Mol. Mutagen.* **1992,** *19*, 37-52; (b) Benigni, R.; Andreoli, C.; Giuliani, A. QSAR models for both mutagenic potency and activity: application to nitroarenes and aromatic amines. *Environ. Mol. Mutagen.* **1994,** *24*, 208-219.

30.   Tichenor, M. S.; Keith, J. M.; Jones, W. M.; Pierce, J. M.; Merit, J.; Hawryluk, N.; Seierstad, M.; Palmer, J. A.; Webb, M.; Karbarz, M. J.; Wilson, S. J.; Wennerholm, M. L.; Woestenborghs, F.; Beerens, D.; Luo, L.; Brown, S. M.; Boeck, M. D.; Chaplan, S. R.; Breitenbucher, J. G. Heteroaryl urea inhibitors of fatty acid amide hydrolase: structure-mutagenicity relationships for arylamine metabolites. *Bioorg. Med. Chem. Lett.* **2012,** *22*, 7357-7362.

31.   Wang, X. J.; Zhang, L.; Krishnamurthy, D.; Senanayake, C. H.; Wipf, P. General solution to the synthesis of *N*-2-substituted 1,2,3-triazoles. *Org. Lett.* **2010,** *12*, 4632-4635.

32.   (a) Barnes-Seeman, D.; Jain, M.; Bell, L.; Ferreira, S.; Cohen, S.; Chen, X. H.; Amin, J.; Snodgrass, B.; Hatsis, P. Metabolically stable tert-butyl replacement. *ACS Med. Chem. Lett.* **2013,** *4*, 514-516; (b) Westphal, M. V.; Wolfstadter, B. T.; Plancher, J. M.; Gatfield, J.; Carreira, E. M. Evaluation of *tert*-butyl isosteres: case studies of physicochemical and pharmacokinetic properties, efficacies, and activities. *ChemMedChem* **2015,** *10*, 461-469.

33.   De Sarro, G.; Russo, E.; Citraro, R.; Meldrum, B. S. Genetically epilepsy-prone rats (GEPRs) and DBA/2 mice: Two animal models of audiogenic reflex epilepsy for the evaluation of new generation AEDs. *Epilepsy Behav.* **2017,** *71* (Pt B), 165-173.

34.   Ellenbogen, K. A.; German, L. D.; O'Callaghan, W. G.; Colavita, P. G.; Marchese, A. C.;

Gilbert, M. R.; Strauss, H. C. Frequency-dependent effects of verapamil on atrioventricular nodal

conduction in man. *Circulation* **1985,** *72*, 344-352.

35.   (a) Hansen, P. B. Functional and pharmacological consequences of the distribution of

voltage-gated calcium channels in the renal blood vessels. *Acta Physiol.* **2013,** *207*, 690-699; (b)

Hansen, P. B. Functional importance of T-type voltage-gated calcium channels in the

cardiovascular and renal system: news from the world of knockout mice. *Am. J. Physiol. Regul.*

Integr. Comp. Physiol. **2015,** *308*, R227-237.

TABLE OF CONTENTS GRAPHIC
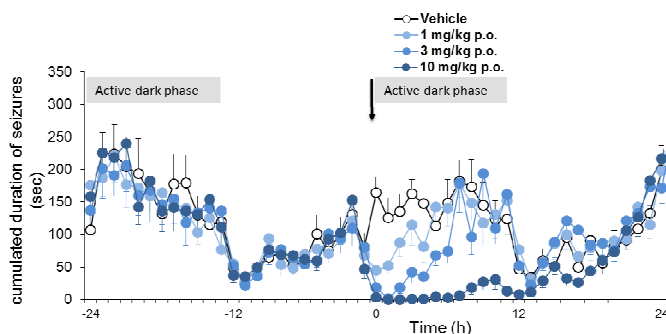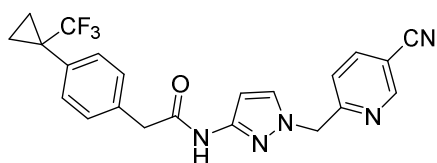
Impacts on the cumulative duration of absence seizures in the male WAG/Rij rats model